國立交通大學

機械工程學系

工學院精密與自動化工程學程

碩 士 論 文

由本身系統之增項及代換達成之 Lorenz 系統超渾沌，渾沌控制及渾沌同步

Hyperchaos and Chaos Control and Synchronization of Lorenz System Obtained by Addition and Replacing of Its Own Chaos and Regular Functions of Time

研究生:林森生

Student: Sen-Sheng Lin

指導教授:戈正銘

Advisor: Zheng-Ming Ge

中華民國九十七年六月

國立交通大學

機械工程學系

碩士論文

由本身系統之增項及代換達成之Lorenz系統超渾沌，渾沌控制及渾沌同步

Hyperchaos and Chaos Control and Synchronization of Lorenz System Obtained by Addition and Replacing of Its Own Chaos and Regular Functions of Time

研究生:林森生 Student: Sen-Sheng Lin

指導教授:戈正銘 Advisor: Zheng-Ming Ge

A Thesis
Submitted to Institute of Mechanical Engineering
College of Engineering
National Chiao Tung University
In Partial Fulfillment of the Requirement
For the Degree of Master of Science
In
Mechanical Engineering
November 2007
Hsinchu, Taiwan, Republic of China

中華民國九十七年六月

由本身系統之增項及代換達成之Lorenz系統超渾沌, 渾沌控制及渾沌同步

研究生：林森生　　　　　　　　　　　　　　　　指導教授：戈正銘

國立交通大學機械工程研究所

摘要

本論文研究超渾沌Lorenz系統藉由其本身渾沌激發而得到。應用以渾沌或規則時間函數代替參數法可得Lorenz系統的渾沌控制與同步。以渾沌或規則時間函數代替參數，也可得Lorenz系統之非耦合渾沌同步。最後應用本身渾沌及規則函數之增項及取代法也可得Lorenz系統之渾沌與渾沌同步。

國立交通大學

論文口試委員會審定書

本校 工學院精密與自動化工程 學程碩士班 林森生 君

所提論文：

由本身系統之增項及代換達成之 Lorenz 系統超渾沌，渾沌控制及渾沌同步

Hyperchaos and Chaos Control and Synchronization of Lorenz System Obtained by Addition and Replacing of Its Own Chaos and Regular Functions of Time

合於碩士資格水準、業經本委員會評審認可。

口試委員：

林宗南　　古富能

陳恒輝

指導教授：戈正銘

班主任：潘樹民

中華民國 97 年 6 月 12 日

Hyperchaos and Chaos Control and Synchronization of Lorenz System Obtained by Addition and Replacing of Its Own Chaos and Regular Functions of Time

Student：Sen-Sheng Lin Advisor：Zheng-Ming Ge

Department of Mechanical Engineering
National Chiao Tung University

ABSTRAST

Hyperchaotic Lorenz system is obtained by replacement of its parameters by its chaotic states. The chaos control, synchronization and uncoupled synchronization of the systems are also obtained by replacement of its parameters by its chaotic states or by regular functions of time. Furthermore, by addition and replacement of its own chaotic states, chaos control and synchronization of Lorenz system can also be obtained.

ACKNOWLEDGMENT

此篇論文及碩士學業之完成，首先，必須感謝指導教授戈正銘老師的循循善誘與敦敦教誨，使我在「渾沌」這個研究領域得以引導入門，讓我在陷入瓶頸時得以漸入佳境。老師對學術研究與詩詞文學創作所投注的那份專注與散發之光彩更是令人覺得仰之彌高,鑽之彌深。此外老師幽默樂觀的處世態度，對傳統戲劇文化的熱愛與隨遇而安的生活更是我效法的楷模。

多年的在職研究生涯讓我得以完成,感謝我的一起跟著我學習與成研究的學長與學弟們,感謝他們在學業與生活上的鼎力相助。感謝張晉民、鄭普建、楊振雄與陳炎生等諸位學長的熱心指導，在研究陷入渾沌的困境時，幫助我走出渾沌的崎嶇道路。此外也感謝研究室其他同學陪我渡過這段日子。

最重要的是要感謝父母與妻子的支持，讓我在工作之餘可以重拾書本利用的休息時間來研究並完成學業。此外必須感謝一起工作過之同仁與推薦之長官，讓我有機會再進修並得以繼續追尋人生的許多大夢，也讓我可以儲備新的能量邁向新的世紀。

CONTENTS：

LIST OF FIGURES：

Chapter 1

Introduction

Chaos has been observed in a lot of nonlinear dynamical systems [1], and it is quite useful in many applications such as heart beat regulation [2], fluid mixing [3], human brain [4], etc. When it is undesirable, chaos control is used [5], while when it is desirable, chaotification is used. During the past decades, chaos synchronization has been applied in many fields such as secure communication [6], chemical and biological systems [7], etc.

Hyperchaotic phenomena and chaos control of Lorenz systems are studied in this thesis. The first hyperchaotic system is hyperchaotic Rössler system [8], after that, many hyperchaotic systems have been found such as the hyperchaotic MCK circuit [9], the hyperchaotic Chen system [10], etc. The above hyperchaotic systems are developed by introducing a new state to the original chaotic systems. Different from that, the hyperchaotic Lorenz system studied here is obtained from excitation by its own chaos. In this thesis, hyperchaos is obtained by replacement of its parameters by its chaotic states. The chaos control, synchronization and uncoupled synchronization of the systems are also obtained by replacement of its parameters by its chaotic states or by regular function of time. Furthermore, by addition and replacement of its own chaotic states, chaos control and synchronization of Lorenz system can also be obtained.

This paper is organized as follows. Chapter 2 contains the hyperchaos of Lorenz system excited by its own chaos. First, the second Lorenz system is excited by the first system. Second, the third Lorenz system is excited by the second system. In Chapter 3, chaos control of Lorenz system is achieved by chaos excitation and excitation of sum of chaos and regular functions of time. In Chapter 4, chaos synchronization will be obtained by replacing parameter by chaotic and regular function of time. In Chapter 5 uncoupled chaos synchronization of two Lorenz systems is obtained by addition and replacement of its own chaotic states.

Chapter 2

Hyperchaos of a Lorenz System Obtained by Additions of Chaos

In order to generate hyperchaotic phenomena of a Lorenz system, two types of excitation are investigated. First, a second Lorenz system is excited by additive chaotic states of the first system. Second, the third Lorenz system is excited by the second system.

2.1 Hyperchaos of a Lorenz System Obtained by Additions of Chaotic States of Its Own System

Chaotic behavior is excited by adding chaotic signals from chaos supply system. The chaos supply system is a Lorenz system:

$$\begin{cases} \dot{x}_1 = -\sigma(x_1 - y_1) \\ \dot{y}_1 = rx_1 - y_1 - x_1 z_1 \\ \dot{z}_1 = x_1 y_1 - bz_1 \end{cases} \tag{2.1}$$

and the chaos excited system is:

$$\begin{cases} \dot{x}_2 = -\sigma(x_2 - y_2) + u_1(t) \\ \dot{y}_2 = rx_2 - y_2 - x_2 z_2 + u_2(t) \\ \dot{z}_2 = x_2 y_2 - bz_2 + u_3(t) \end{cases} \tag{2.2}$$

Rewrite Eqs. (2.1) and Eqs. (2.2) as:

$$
\begin{cases}
\dot{x}_1 = -\sigma(x_1 - y_1) \\
\dot{y}_1 = rx_1 - y_1 - x_1 z_1 \\
\dot{z}_1 = x_1 y_1 - b z_1 \\
\dot{x}_2 = -\sigma(x_2 - y_2) + u_1(t) \\
\dot{x}_2 = -rx_2 - y_2 - x_2 z_2 + u_2(t) \\
\dot{z}_2 = x_2 y_2 - b z_2 + u_3(t)
\end{cases}
\qquad \textbf{(2.3)}
$$

where σ=36, r=3, b=20, and the initial condition are x_1(0)=0.001, y_1(0)=0.001, z_1(0)=0, x_2 (0)=0.001, y_2(0)=0.001, z_2(0)=0.

(1) $u_1(t) = 0, u_2(t) = 0, u_3(t) = Az_1$

Six Lyapunov exponents for system (2.3) are shown in Fig. 2.1 in which three black horizontal lines are the Lyapunov exponents of system (2.1), three remained colored curves are Lyapunov exponents of system (2.2). The phase portraits system (2.2) where $u_1(t) = 0, u_2(t) = 0, u_3(t) = -2z_1$ are shown in Fig. 2.2. When -100<A<0, there are two positive Lyapunov exponents as shown in Fig 2.1. Hyperchaos is obtained.

(2) $u_1(t) = 0, u_2(t) = 0, u_3(t) = Ay_1$

The Lyapunov exponents for system (2.3) with $u_1(t) = 0, u_2(t) = 0, u_3(t) = Ay_1$ are shown in Fig. 2.3. The local enlargement of Fig. 2.3 is shown in Fig. 2.4. When -1.5<A<1.5 hyperchaos occasionally appears.

(3) $u_1(t) = Ay_1, u_2(t) = 0, u_3(t) = 0$

The Lyapunov exponents for system (2.3) are shown in Fig. 2.5. The local enlargement of Fig. 2.5 is shown in Fig. 2.6. When -0.3<A<0.3 hyperchaos occasionally appears.

(4) $u_1(t) = 0, u_2(t) = Ay_1, u_3(t) = 0$, $A = -20 \sim 20$

The Lyapunov exponents for system (2.3) are shown in Fig. 2.7. The local enlargement of Fig. 2.7 is shown in Fig. 2.8. When -0.7<A<0.7, hyperchaos appears frequently.

(5) $u_1(t) = x_1, u_2(t) = 0, u_3(t) = Az_1$

The Lyapunov exponents for system (2.3) are shown in Fig. 2.9. The local enlargement of Fig.

2.9 is shown in Fig. 2.10. When $1.7<A < 2.4$, hyperchaos appears always.

From the above five cases, it is tentatively concluded that the more additive chaotic terms, the more hyperchaos.

2.2 Hyperchaos of a Lorenz System Excited by Double Additive Chaotic States of Chaotic Lorenz System

Hyperchaotic is excited by additive chaotic states of excited Lorenz system. The chaos supply system is a Lorenz system:

$$\begin{cases} \dot{x}_1 = -\sigma(x_1 - y_1) \\ \dot{y}_1 = rx_1 - y_1 - x_1 z_1 \\ \dot{z}_1 = x_1 y_1 - bz_1 \end{cases} \tag{2.4}$$

and the first chaos excited system is:

$$\begin{cases} \dot{x}_2 = -\sigma(x_2 - y_2) + u_1(t) \\ \dot{y}_2 = rx_2 - y_2 - x_2 z_2 + u_2(t) \\ \dot{z}_2 = x_2 y_2 - bz_2 + u_3(t) \end{cases} \tag{2.5}$$

and the second chaos excited system is:

$$\begin{cases} \dot{x}_3 = -\sigma(x_2 - y_2) + v_1(t) \\ \dot{y}_3 = rx_2 - y_2 - x_2 z_2 + v_2(t) \\ \dot{z}_3 = x_2 y_2 - bz_2 + v_3(t) \end{cases} \tag{2.6}$$

Rewrite Eqs. (2.4), Eqs. (2.5) and Eqs.(2.6) as:

$$\begin{cases} \dot{x}_1 = -\sigma(x_1 - y_1) \\ \dot{y}_1 = rx_1 - y_1 - x_1 z_1 \\ \dot{z}_1 = x_1 y_1 - bz_1 \\ \dot{x}_2 = -\sigma(x_2 - y_2) + u_1(t) \\ \dot{y}_2 = rx_2 - y_2 - x_2 z_2 + u_2(t) \\ \dot{z}_2 = x_2 y_2 - bz_2 + u_3(t) \\ \dot{x}_3 = -\sigma(x_3 - y_3) + v_1(t) \\ \dot{y}_3 = rx_3 - y_3 - x_3 z_3 + v_2(t) \\ \dot{z}_3 = x_3 y_3 - bz_3 + v_3(t) \end{cases} \qquad \textbf{(2.7)}$$

where σ =36, r =3, b =20, and the initial conditions are x_1(0)=0.002, y_1(0)=0.001, z_1(0)=0.003, x_2(0)=0.004, y_2(0)=0.002, z_2(0)=0.001, x_3(0)=0.001, y_3(0)=0.002, z_3(0)=0.001

(1) $u_1(t) = 0, u_2(t) = Ax_1, u_3(t) = 0, v_1(t) = 0, v_2(t) = Ax_2, v_3(t) = 0$

The Lyapunov exponents for systems (2.7) are shown in Fig. 2.11. The local enlargement of Fig. 2.11 is shown in Fig. 2.12. When 40<A<100, hyperchaos occurs.

(2) $u_1(t) = 0, u_2(t) = 0, u_3(t) = Ax_1, v_1(t) = 0, v_2(t) = 0, v_3(t) = Ax_2$

The Lyapunov exponents for system (2.7) are shown in Fig. 2.13. The local enlargement of Fig. 2.13 is shown in Fig. 2.14. When 0<A<1.2, hyperchaos occurs.

(3) $u_1(t) = 0, u_2(t) = 0, u_3(t) = Az_1, v_1(t) = 0, v_2(t) = 0, v_3(t) = x_2 z_2$

The Lyapunov exponents for system (2.7) are shown in Fig. 2.15. The local enlargement of Fig. 2.15 is shown in Fig. 2.16. When -0.3<A<0.3, 2.1<A, 2.3, hyperchaos occurs.

From the above three cases, the hyperchaos of case (1) is most abundant.

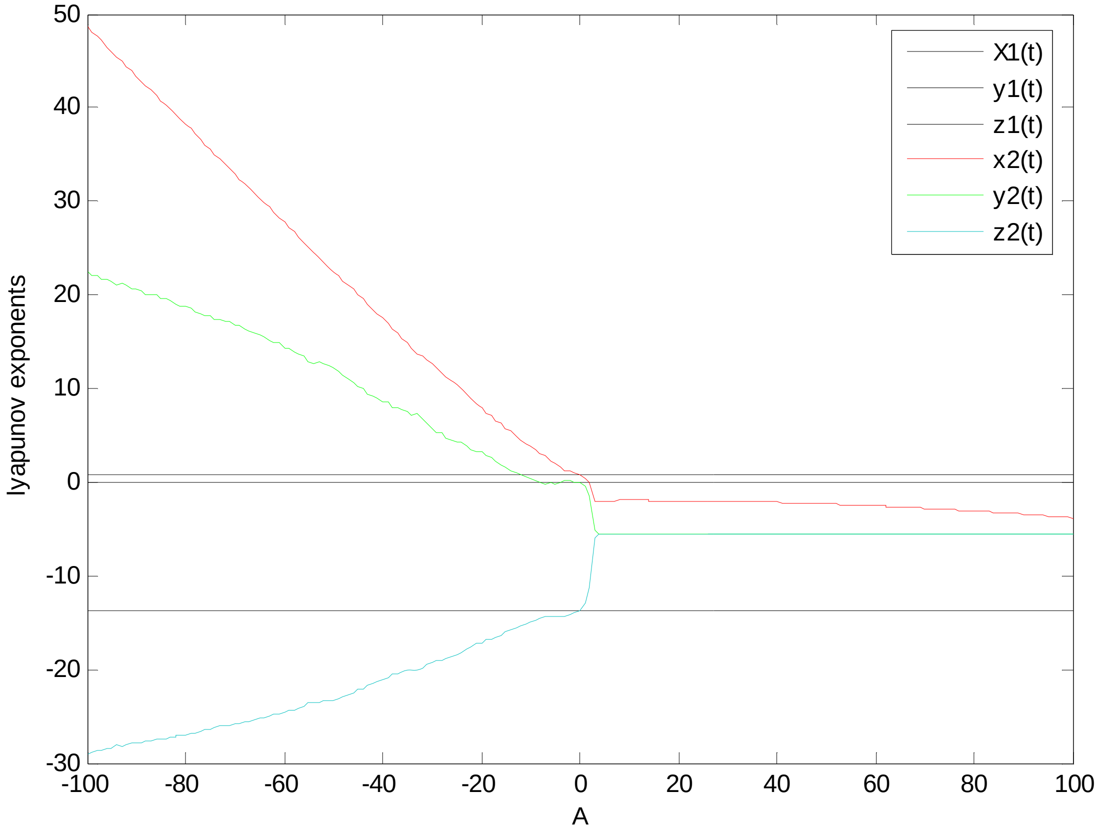

Fig.2. 1 The Lyapunov exponents for system (2.3), where $u_1(t)=0, u_2(t)=0, u_3(t)=Az_1$, $A=-100\sim100$.

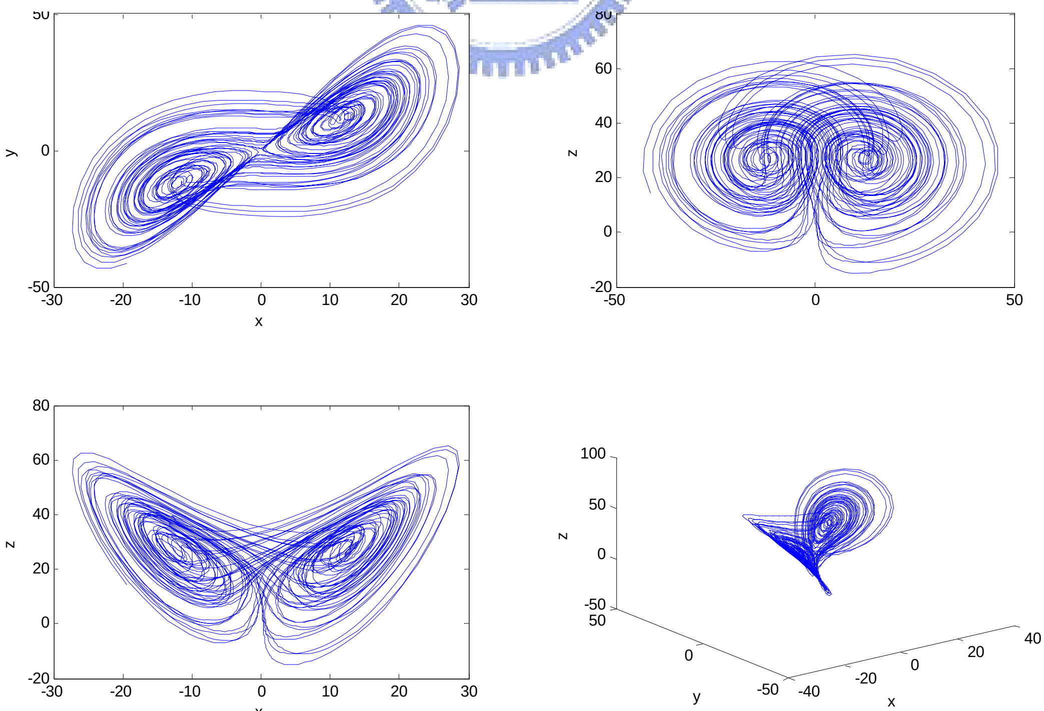

Fig.2. 2 Phase portraits of excited system (2.2) where $u_1(t)=0, u_2(t)=0, u_3(t)=-2z_1$.

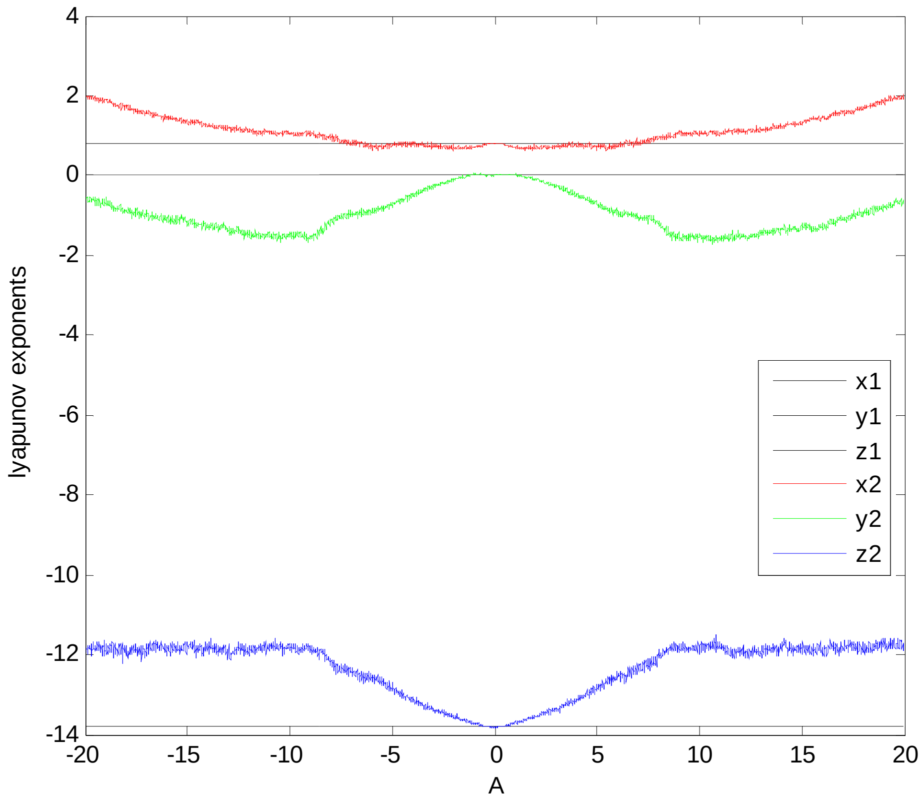

Fig.2. 3 Lyapunov exponents for system (2.3), where $u_1(t) = 0, u_2(t) = 0, u_3(t) = Ay_1, A = -20 \sim 20$.

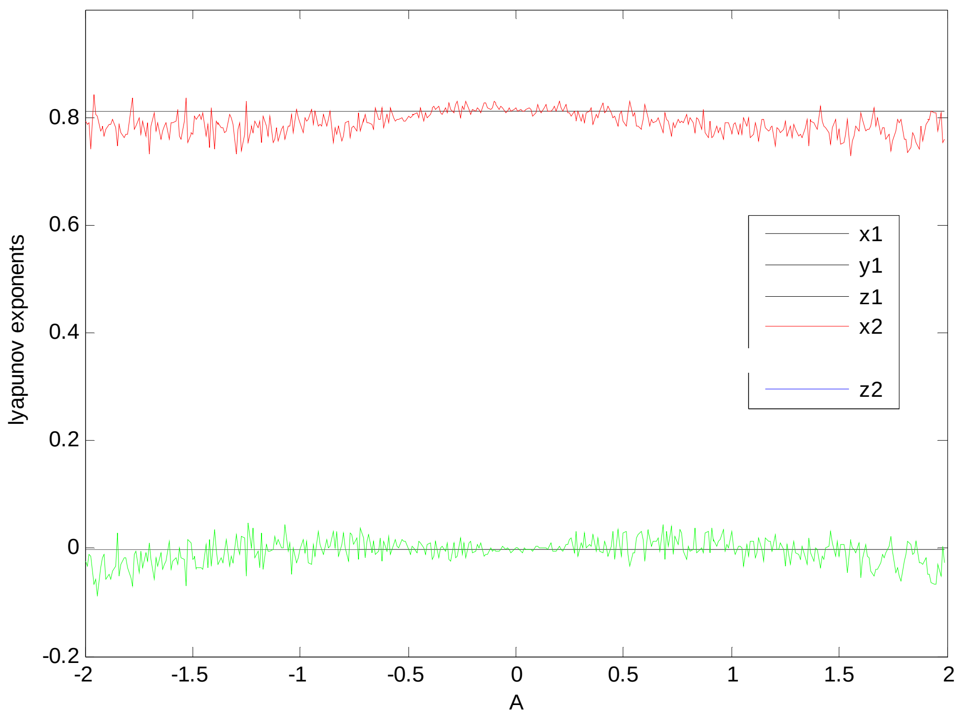

Fig.2. 4 Local enlargement of Fig. 2.3.

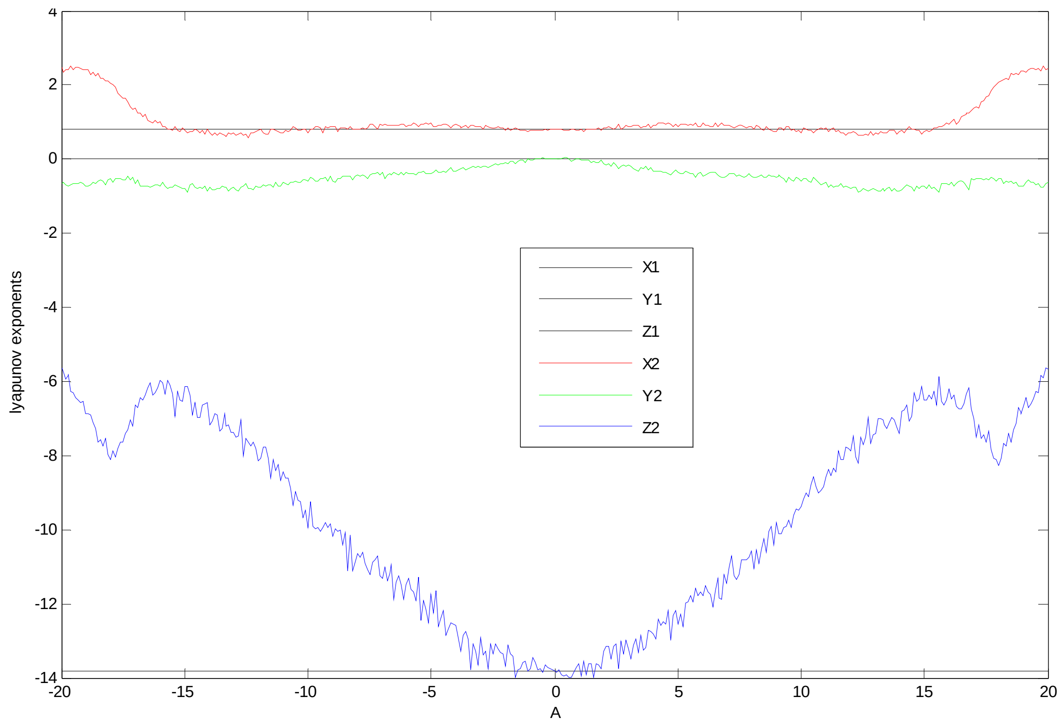

Fig.2. 5 Lyapunov exponents for system (2.3), where $u_1(t) = Ay_1, u_2(t) = 0, u_3(t) = 0, A = -20 \sim 20$.

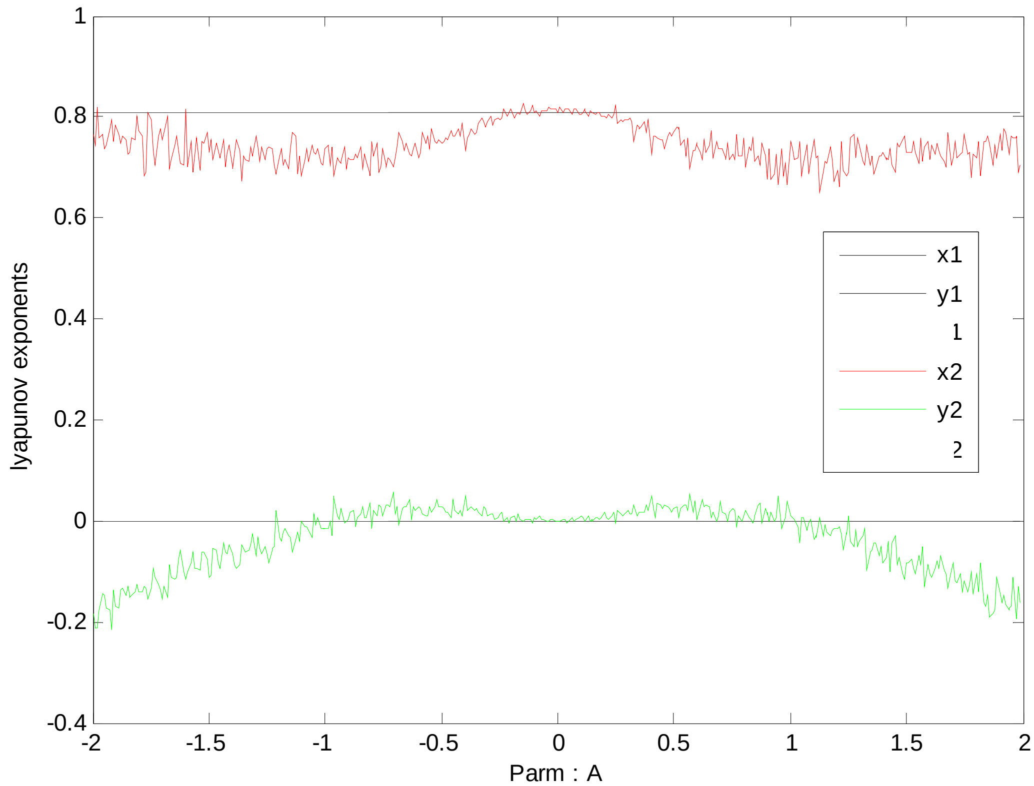

Fig.2. 6 Local enlargement of Fig. 2.5.

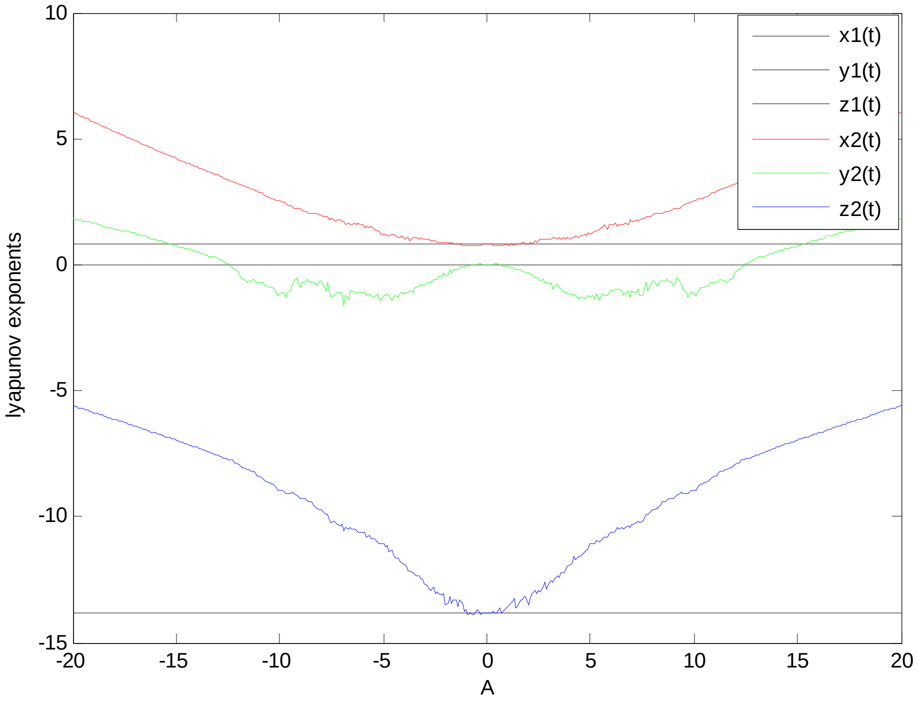

Fig.2. 7 Lyapunov exponents for system (2.3), where $u_1(t)=0, u_2(t)=Ay_1, u_3(t)=0$ $A=-20\sim 20$.

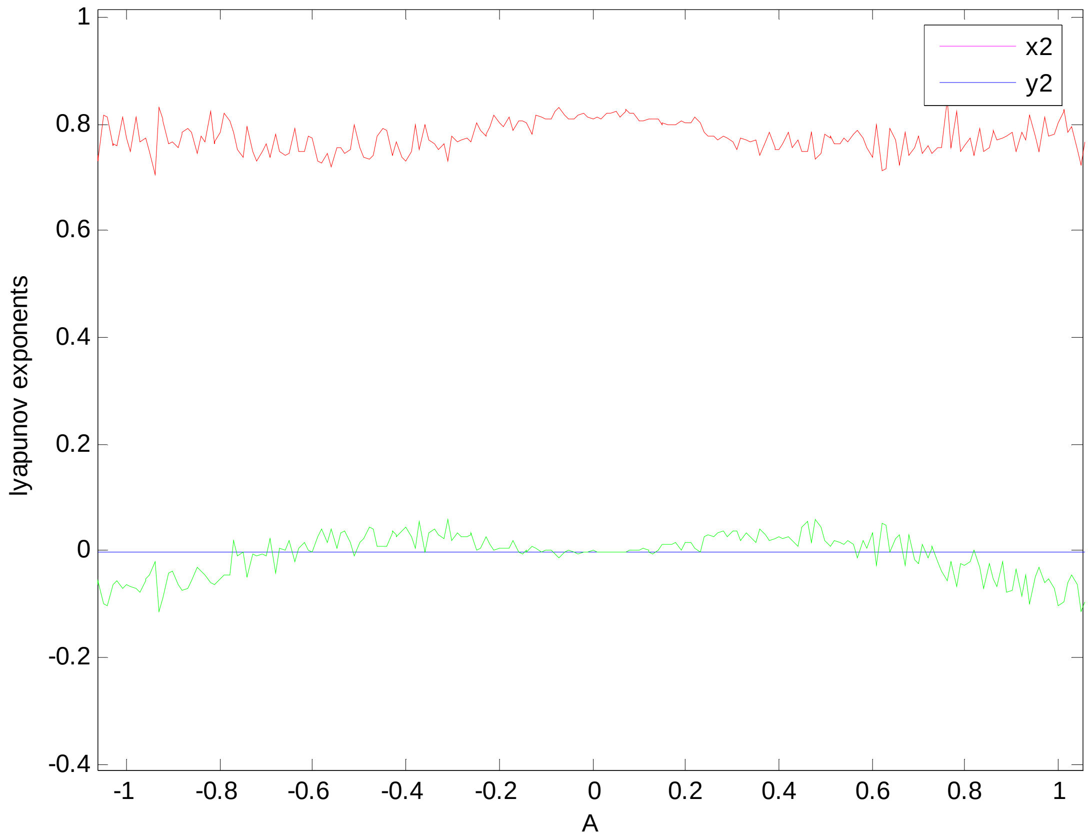

Fig.2. 8 Local enlargement of Fig. 2.7.

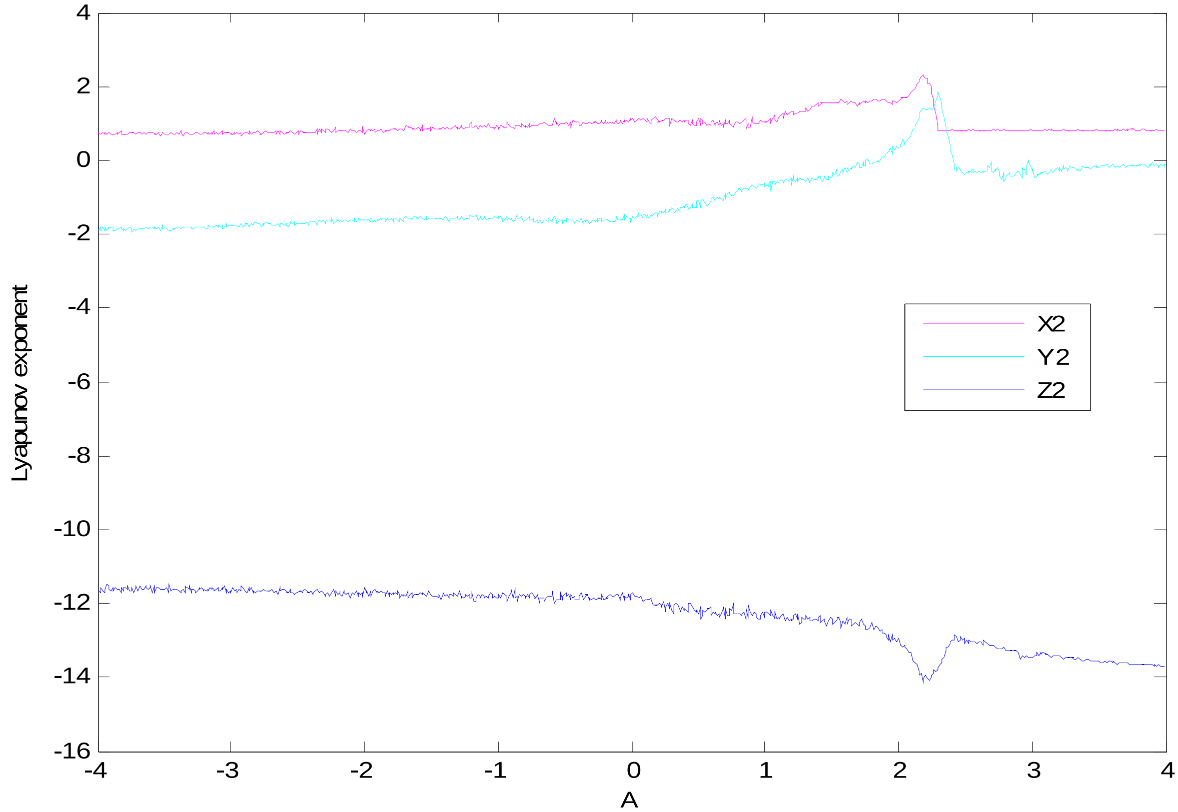

Fig.2. 9 Lyapunov exponents for system (2.3) , where $u_1(t) = x_1, u_2(t) = 0, u_3(t) = Az_1, A = -4 \sim 4$.

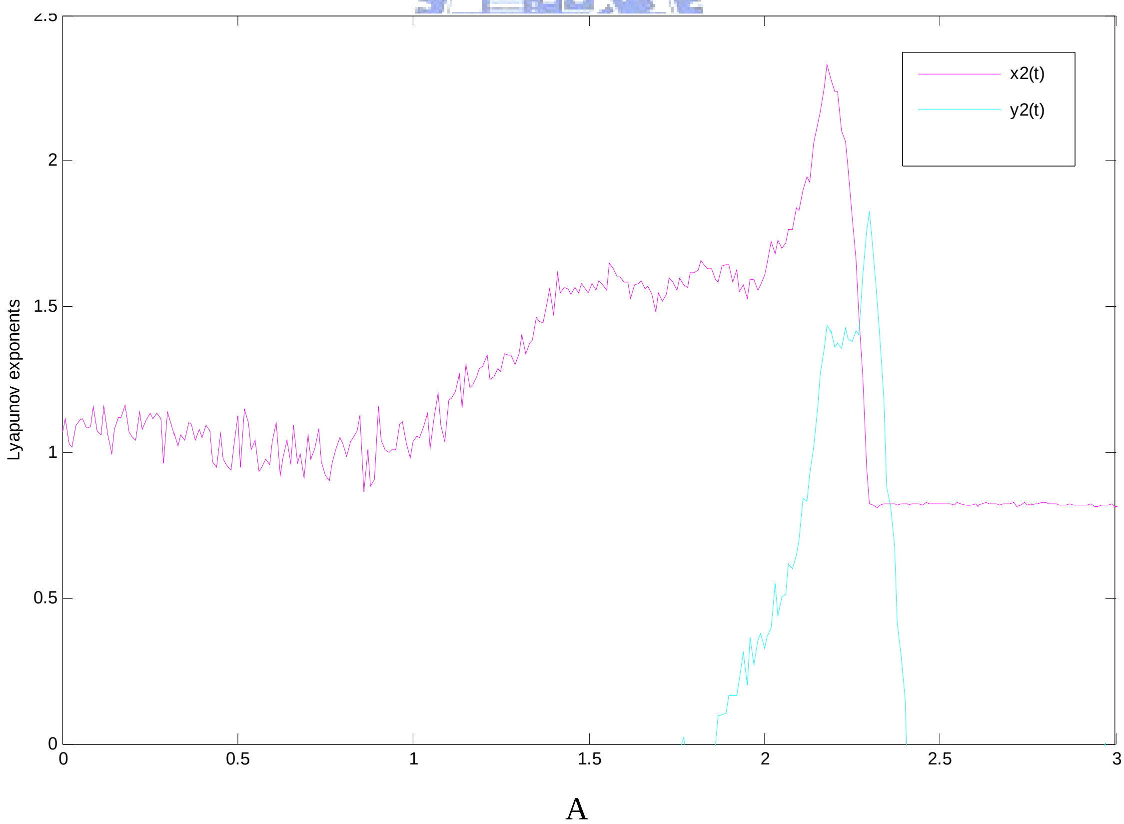

Fig.2. 10 Local enlargement of Fig. 2.9.

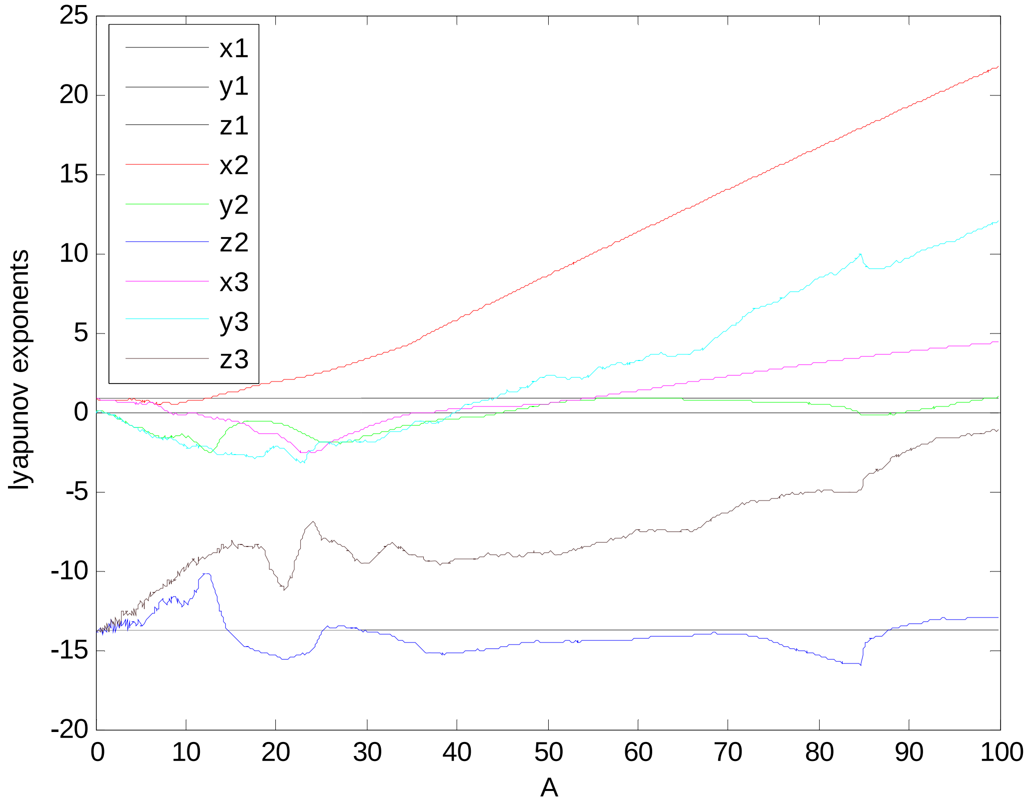

Fig.2. 11 Lyapunov exponents for system (2.7), where
$u_1(t) = 0, u_2(t) = Ax_1, u_3(t) = 0, v_1(t) = 0, v_2(t) = Ax_2, v_3(t) = 0, A = 0 \sim 100$.

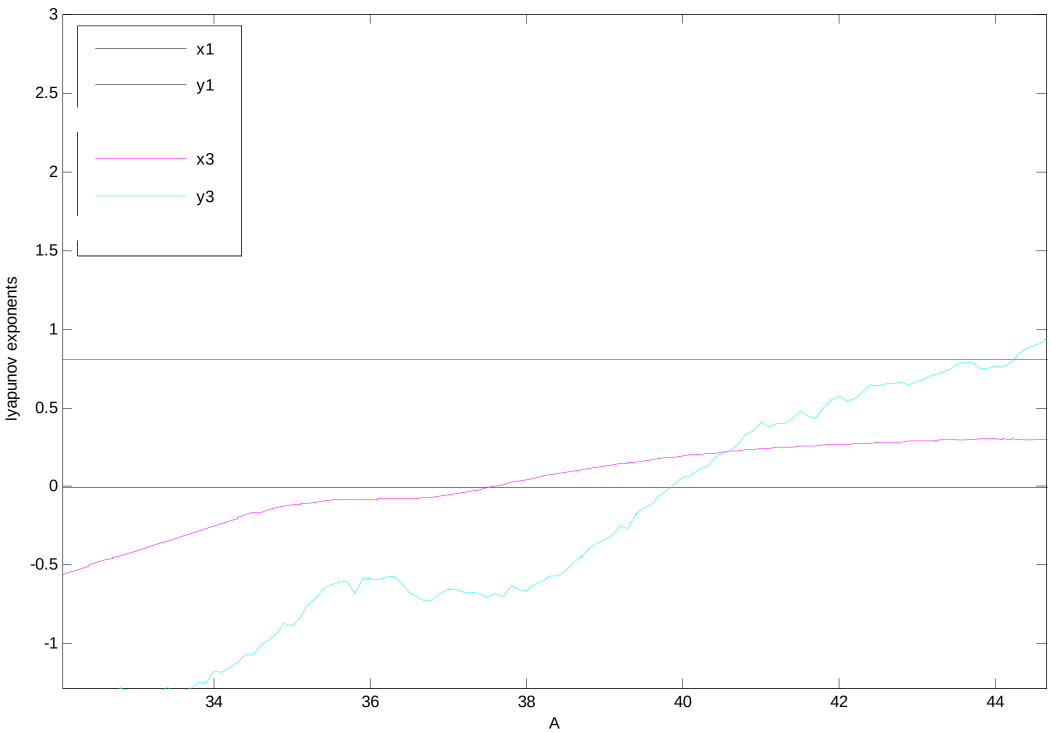

Fig.2. 12 Local enlargement of Fig. 2.12.

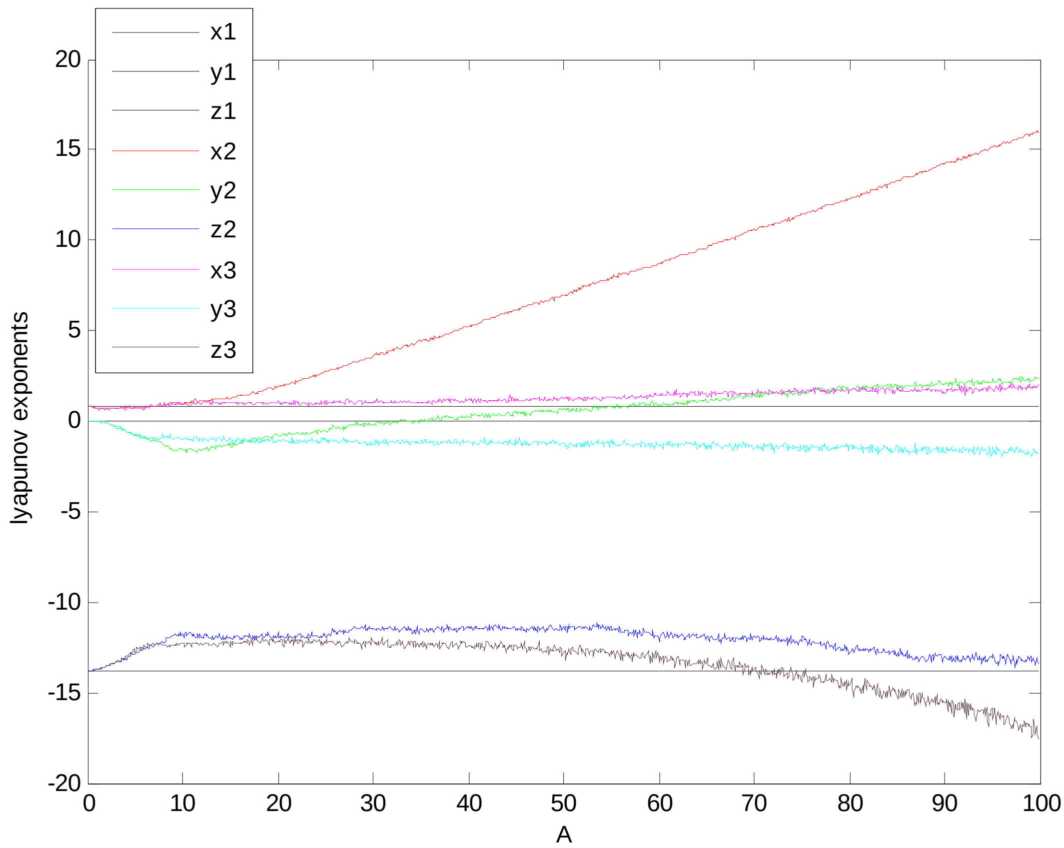

Fig.2. 13 Lyapunov exponents for system (2.7), where
$u_1(t)=0, u_2(t)=0, u_3(t)=Ax_1, v_1(t)=0, v_2(t)=0, v_3(t)=Ax_2, A=0\sim100$.

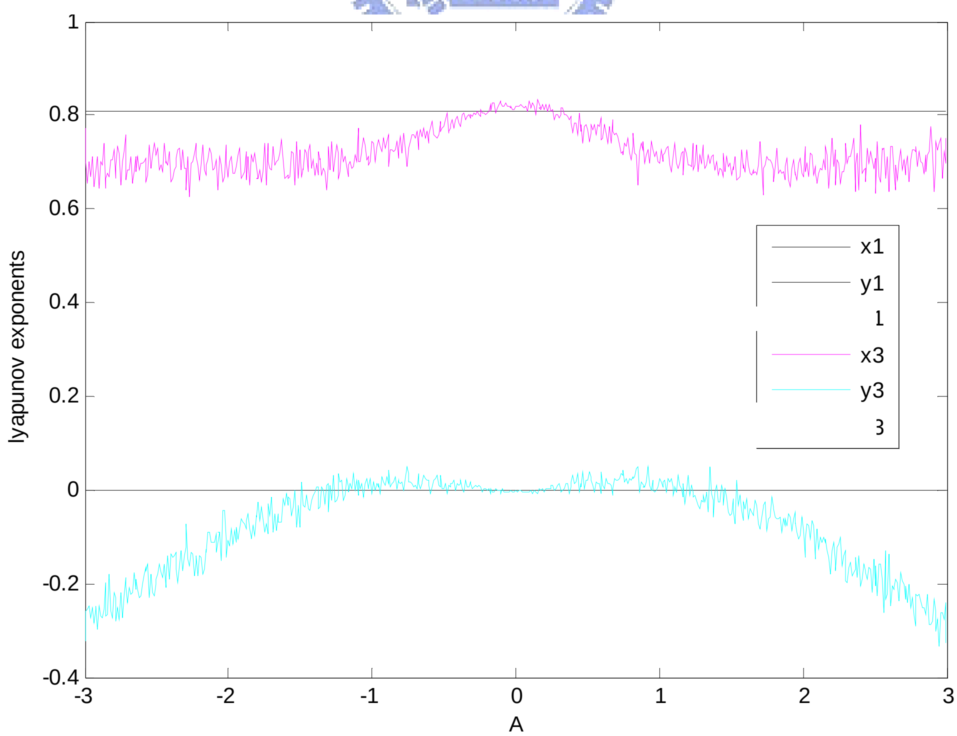

Fig.2. 14 Local enlargement of Fig. 2.13.

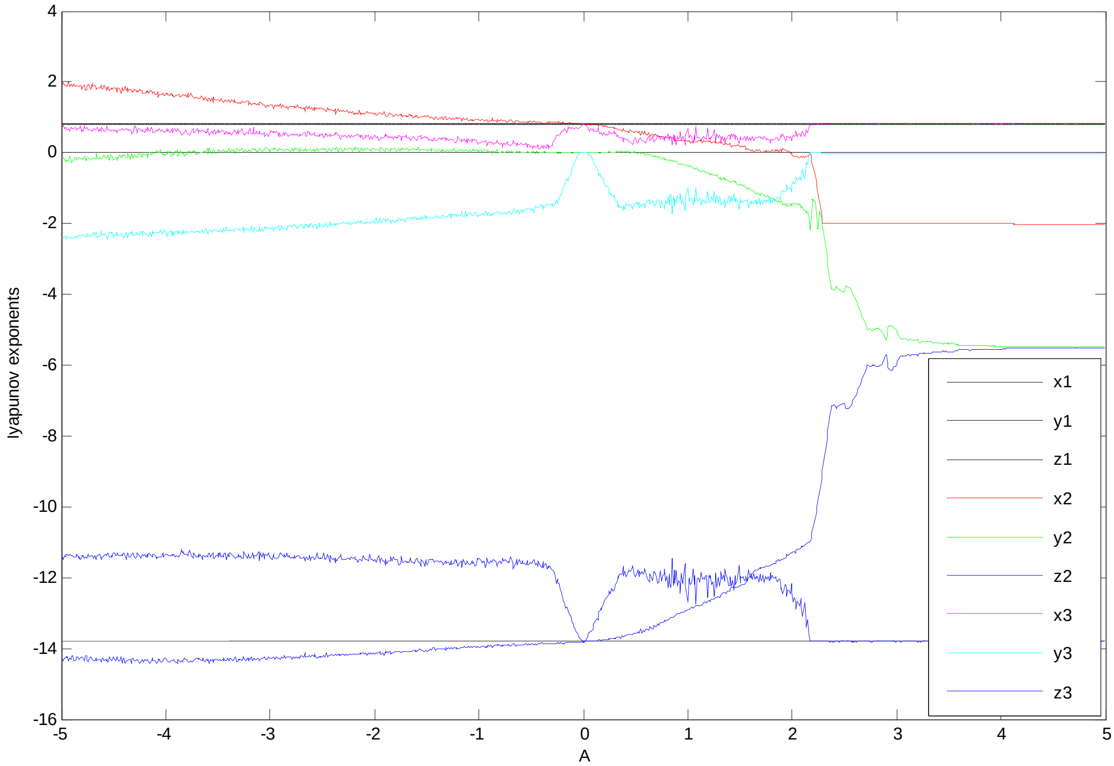

Fig.2. 15 Lyapunov exponents for system (2.7), where
$u_1(t)=0, u_2(t)=0, u_3(t)=Az_1, v_1(t)=0, v_2(t)=0, v_3(t)=x_2z_2, A=-5\sim 5.$

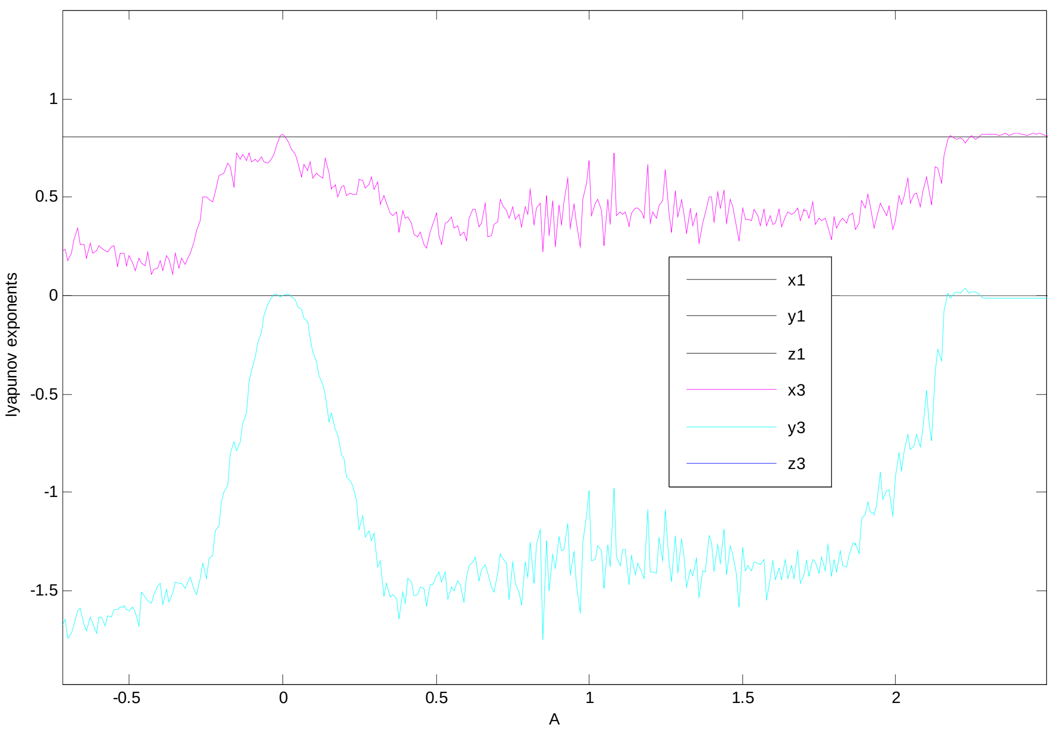

Fig.2. 16 Local enlargement of Fig. 2.15.

Chapter 3

Chaos Control by Replacing Parameter by Chaotic States

In this Chapter, chaos control of a Lorenz system is achieved by chaos excitation and excitation of sum of chaos and regular functions of time.

3.1 Chaos Control of a Lorenz System by Replacing Parameters with Chaos

In order to control the chaos of a Lorenz system, some parameters of Lorenz system are replaced by chaotic signals from a chaos supply system which is also a Lorenz system:

$$\begin{aligned} \dot{x}_1 &= -\sigma(x_1 - y_1) \\ \dot{y}_1 &= r x_1 - y_1 - x_1 z_1 \\ \dot{z}_1 &= x_1 y_1 - b z_1 \end{aligned} \qquad \textbf{(3.1)}$$

For Eqs. (3.1) with σ =36, r =3, b =20, the initial condition are $x_1(0)$ = 0.001, $y_1(0)$ = 0.002, $z_1(0)$ = 0. The chaos excited Lorenz system is:

$$\begin{aligned} \dot{x}_2 &= -\sigma'(t)(x_2 - y_2) \\ \dot{y}_2 &= r'(t) x_2 - y_2 - x_2 z_2 \\ \dot{z}_2 &= x_2 y_2 - b'(t) z_2 \end{aligned} \qquad \textbf{(3.2)}$$

For Eqs. (3.2), the initial conditions are $x_2(0)$ = 0.001, $y_2(0)$ = 0.002, $z_2(0)$ = 0.001, and $\sigma'(t)$, $r'(t)$, $b'(t)$ are the chaotic parameters formed by chaotic states of system (3.1).

For $\sigma'(t) = \sigma$, $r'(t) = r$, $b'(t) = x_1 + 20y_1$ the phase portrait of x_2, y_2, z_2 is shown in Fig 3.1, which converges to a fix point (0,0,8.3351).

For $\sigma'(t) = \sigma, r'(t) = r, b'(t) = |kx_1 + p|$, with $k = 95, p = 0.1$, the phase portrait is shown in Fig. 3.2, which converges to a fix point (506.2837, 506.5360, 29.5925).

For Eqs. (3.1) with σ =36, r =3, b =20, the initial condition are $x_1(0)$ = 1.001, $y_1(0)$ = 1.002,

$z_1(0)$ = 1. For Eqs. (3.2), the initial conditions are $x_2(0)$ = 0.001, $y_2(0)$ = 0.002, $z_2(0)$ = 0.001, and $\sigma'(t)$, $r'(t)$, $b'(t)$ are the chaotic parameters formed by chaotic states of system (3.1).

For $\sigma'(t)=\sigma, r'(t)=|kx_1+p|, b'(t)=b$ with $k=0.01, p=0.1$, the phase portrait is shown in Fig. 3.3, which converges to fixed point (0, 0, 0).

For $\sigma'(t)=|kx_1+p|, r'(t)=r, b'(t)=b$, with $k=0.01, p=0.1$, the phase portrait is shown in Fig 3.4, which converges to fixed point (8.4853, 8.4853, 27).

For $\sigma'(t)=\sigma, r'(t)=r, b'(t)=b+k\sin(\omega t+p)$, with k=0.01, $\omega=1, p=0.1$ the phase portrait is shown in Fig 3.5, which converges to a fixed point (0.00024, 0.00042, 0.6899).

3.2 Chaos Control of a Lorenz System by Replacing a Parameter with Sum of Chaos and Regular Functions of Time

In order to control the chaos of a Lorenz system, a given parameter of Lorenz system are replaced by the sum of chaotic signals from chaos supply system, and regular function of time. The chaos supply system is also a Lorenz system:

$$\begin{cases} \dot{x}_1 = -\sigma(x_1 - y_1) \\ \dot{y}_1 = rx_1 - y_1 - x_1 z_1 \\ \dot{z}_1 = x_1 y_1 - bz_1 \end{cases} \tag{3.3}$$

where σ=36, r=3, b=20, and the initial conditions are $x_1(0)$ = 0.001, $y_1(0)$ = 0.002, $z_1(0)$ = 0. The Lorenz system with parameter replaced by sum of chaos and regular function of time is:

$$\begin{cases} \dot{x}_2 = -\sigma'(t)(x_2 - y_2) \\ \dot{y}_2 = r'(t)x_2 - y_2 - x_2 z_2 \\ \dot{z}_2 = x_2 y_2 - b'(t)z_2 \end{cases} \tag{3.4}$$

where the initial conditions are $x_2(0)$ = 0.001, $y_2(0)$ = 0.002, $z_2(0)$=0.001, r'(t), is the parameter replaced by sum of chaos and regular functions of time, while σ', b' remain unchanged :

$\sigma'(t) = \sigma,\ r'(t) = 10\sin(0.5t) + 10x_1 + y_1,\ b'(t) = b$

The phase portrait, are shown in Fig. 3.6, which is a periodic function of time.

For $\sigma'(t) = \sigma, r'(t) = r, b'(t) = 1.1\sin(0.5t) + 0.1x_1 + 19.5y_1$ the phase portrait is shown in Fig. 3.7, which converges to a fixed point (0, 0, 8.335).

For $\sigma'(t) = |A\sin(\omega t+p)|,\ r'(t) = r,\ b'(t) = b$ and A=200, $\omega = 1, p = 0.1$, the phase portrait is shown in Fig. 3.8, which converges to a fixed point (0, 0, 8.335).

When A=10.5, $\omega = 1.5, p = 1$ the phase portrait is shown in Fig. 3.9, which converges to a fixed point (0, 0, 8.335).

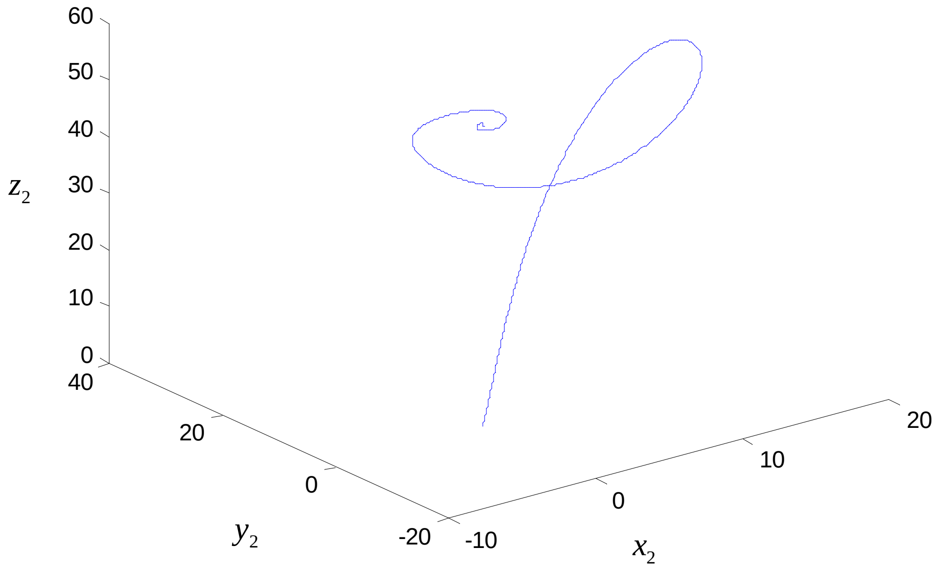

Fig.3. 1 Phase portrait of x_2, y_2, z_2 with $\sigma'(t) = \sigma, r'(t) = r, b'(t) = x_1 + 20y_1$.

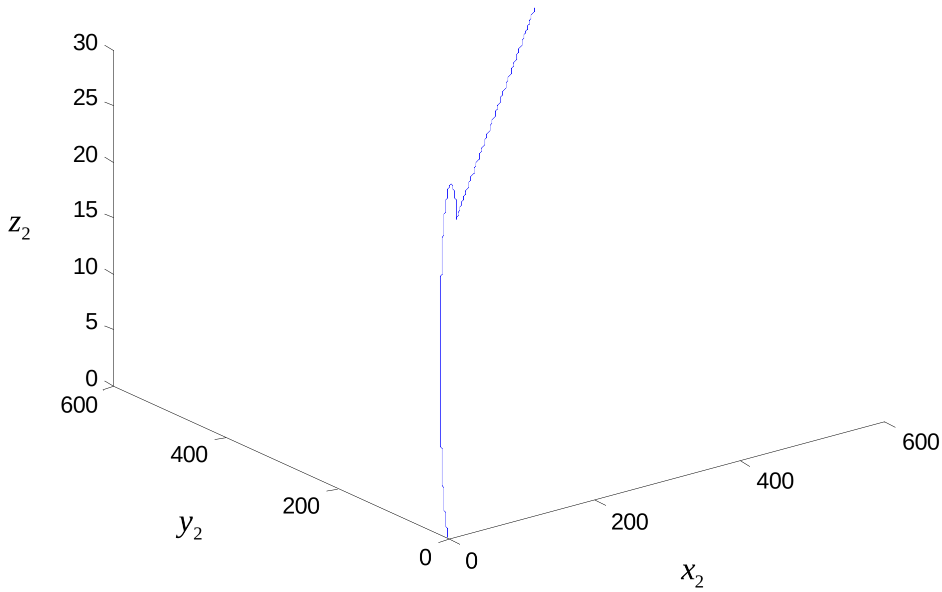

Fig.3. 2 Phase portrait of x_2, y_2, z_2 with $\sigma'(t) = \sigma, r'(t) = r, b'(t) = |95x_1 + 0.1p|$

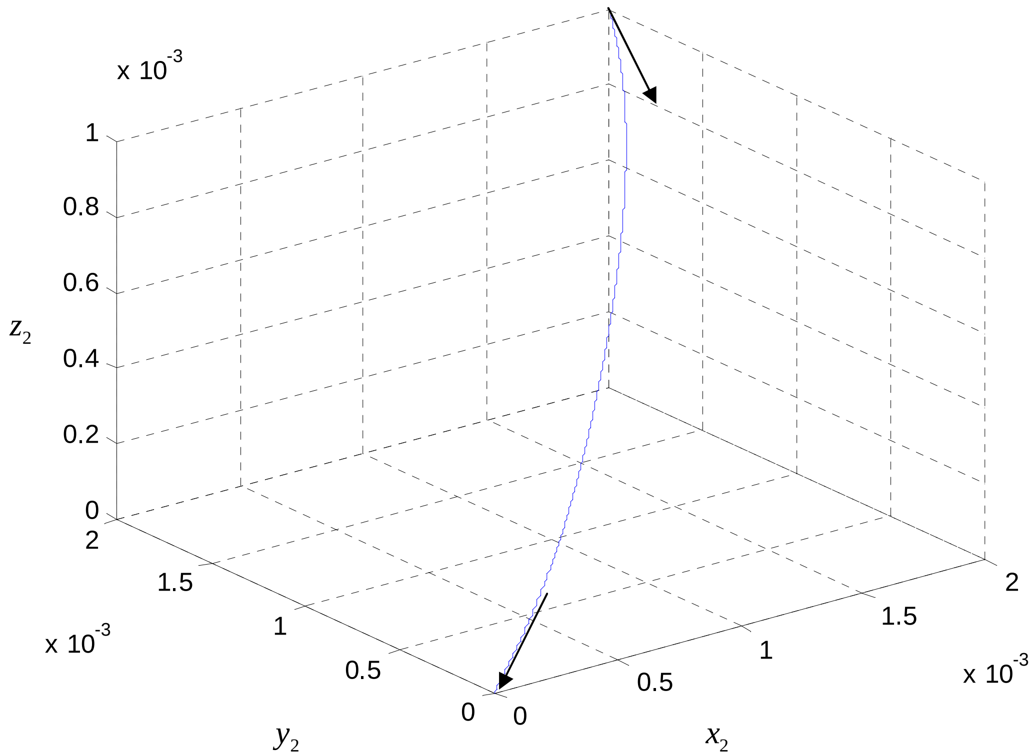

Fig.3. 3 Phase portrait of x_2, y_2, z_2 $\sigma'(t)=\sigma, r'(t)=|0.01x_1+0.1|, b'(t)=b(t)$

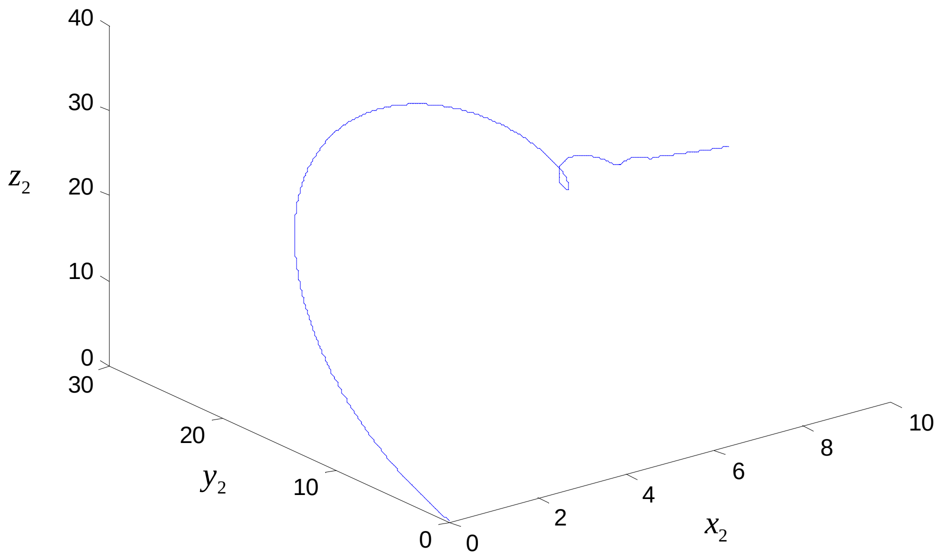

Fig.3. 4 Phase portrait of x_2, y_2, z_2 $\sigma'(t)=|0.01x_1+0.1|, r'(t)=r(t), b'(t)=b(t)$

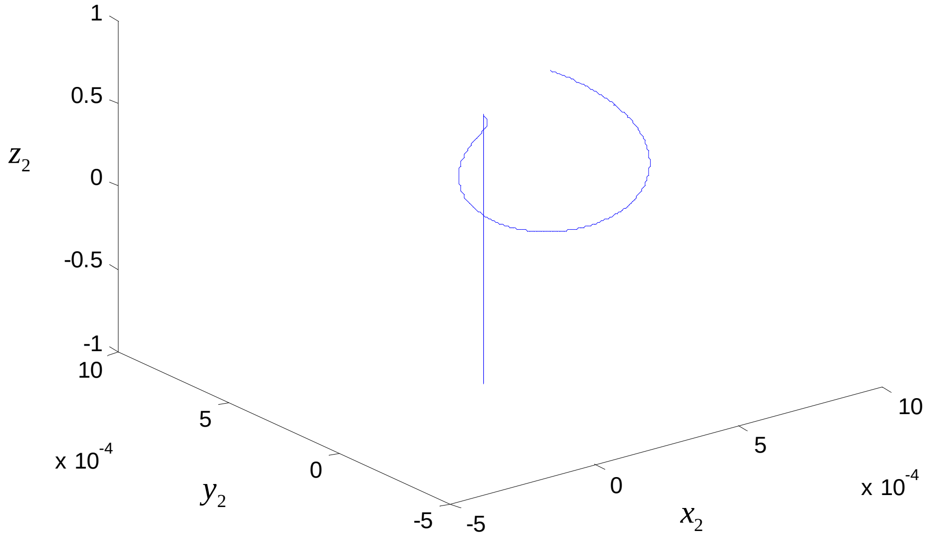

Fig.3. 5 Phase portrait of x_2, y_2, z_2 $\sigma'(t) = \sigma, r'(t) = r(t), b'(t) = b(t) + 0.01\sin(t + 0.1)$

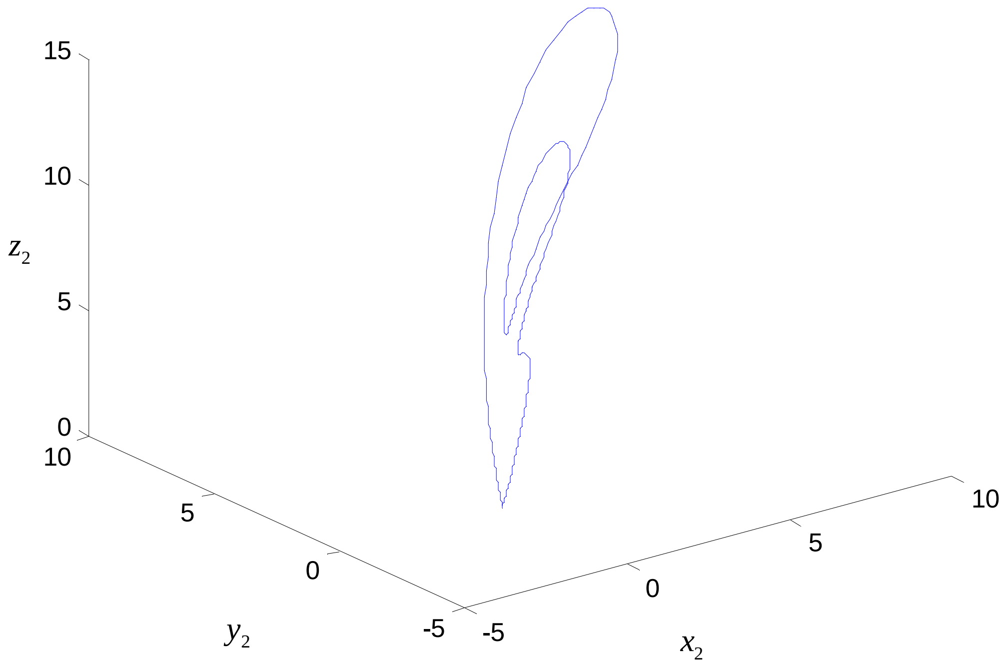

Fig.3. 6 Phase portrait of x_2, y_2, z_2 for $\sigma'(t) = \sigma, r'(t) = 10\sin(0.5t) + 10x_1 + y_1, b'(t) = b$.

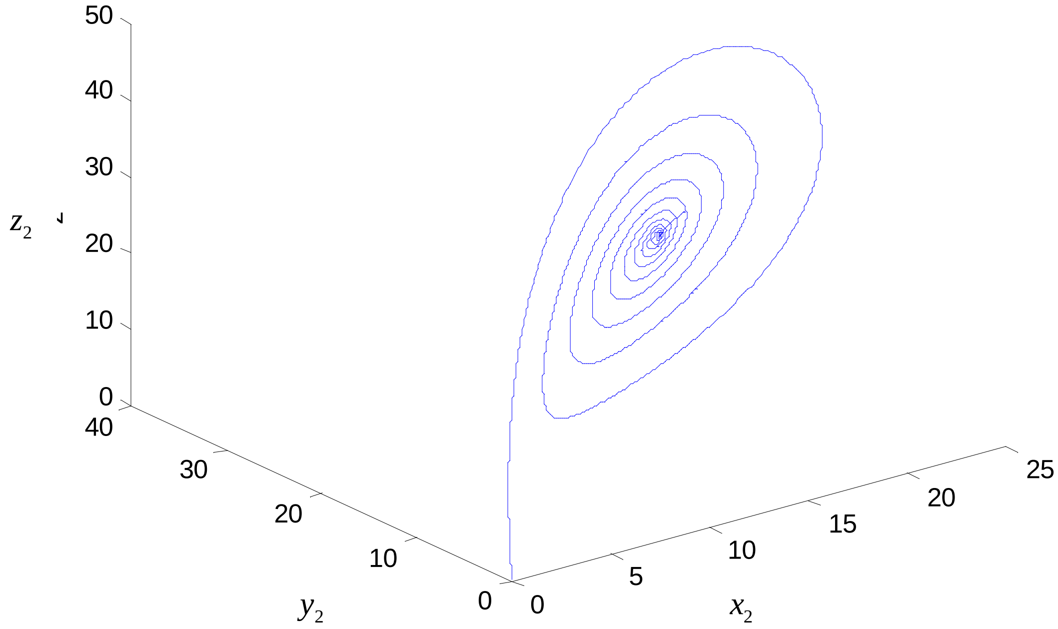

Fig.3. 7 Phase portrait of x_2, y_2, z_2 for $\sigma'(t)=\sigma, r'(t)=r, b'(t)=1.1\sin(0.5t)+0.1x_1+19.5y_1$.

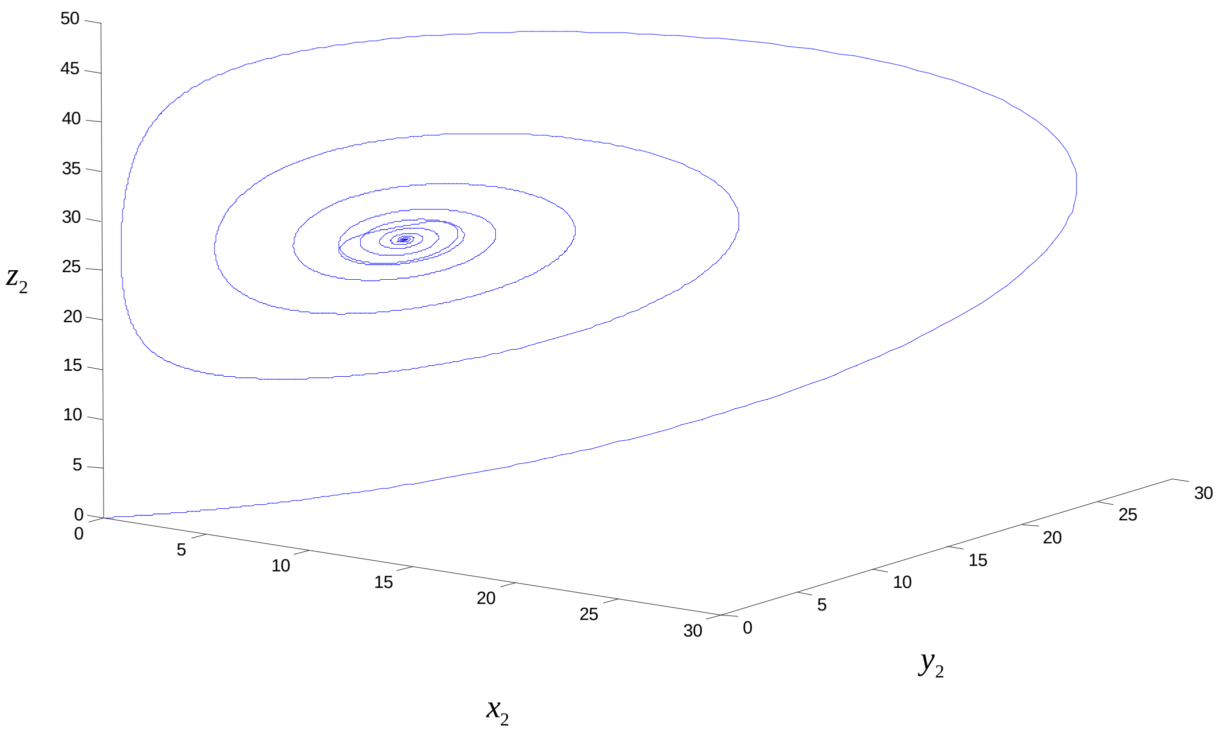

Fig.3. 8 Phase portrait of x_2, y_2, z_2 for $\sigma'(t)=|200\sin(t+0.1)|, r'(t)=r, b'(t)=b$.

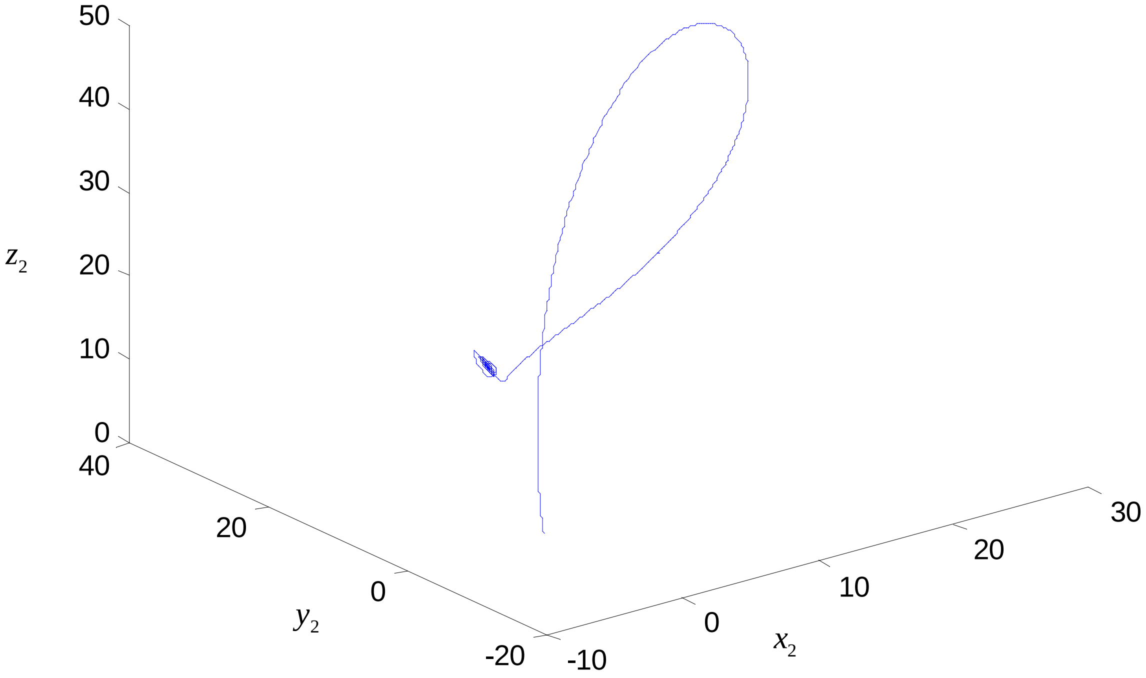

Fig.3. 9 Phase portrait of x_2, y_2, z_2 for $\sigma'(t) = |10.5\sin(1.5t+0.1)|$, $r'(t) = r$, $b'(t) = b$.

Chapter 4

Chaos Synchronization of Two Lorenz Systems by Replacing Parameter and States by Chaotic and Regular Motion

4.1 Chaos synchronization of Lorenz Systems by Replacing a Parameter with Regular Functions of Time

In order to synchronization the chaos of two Lorenz systems, a given parameter of Lorenz system are replaced by regular function of time. Two Lorenz systems are :

$$\begin{cases} \dot{x}_1 = -\sigma(x_1 - y_1) \\ \dot{y}_1 = rx_1 - y_1 - x_1 z_1 \\ \dot{z}_1 = x_1 y_1 - bz_1 \end{cases} \tag{4.1}$$

$$\begin{cases} \dot{x}_2 = -\sigma'(x_2 - y_2) \\ \dot{y}_2 = r' x_2 - y_2 - x_2 z_2 \\ \dot{z}_2 = x_2 y_2 - b'(t) z_2 \end{cases} \tag{4.2}$$

For Eqs.(4.1) with $\sigma = 36$, $r = 3$, $b = 20$, where the initial conditions $x_1(0) = 0.001$, $y_1(0) = 0.002$, $z_1(0) = 0$, $x_2(0) = 0.001$ $y_2(0) = 0.001$, $z_2(0)=0.001$, $b'(t)$ is the parameters replaced by regular functions of time, while σ' , r' remain unchanged . And we define $e_1 = x_2 - x_1$, $e_2 = y_2 - y_1$, $e_3 = z_2 - z_1$.

For $\sigma' = \sigma$, $r' = r$, $b'(t) = b(t) = |k \sin(\omega t + p)|$, $\omega = 1$, $k = 10$, $p = 0.5$, chaos synchronization is obtained as shown in Fig. 4.1 and Fig. 4.2.

For $\sigma' = \sigma$, $r' = r$, $b'(t) = b(t) = |k \sin(\omega t + p)|$, with $\omega = 1.5$, $k = 5$, $p = 0.1$, two systems are synchronized; the time histories and the phase portrait are shown in Fig. 4.3, Fig.4.4.

4.2. Chaos synchronization of a Lorenz System by Replacing some Parameter and States with Chaotic state

In order to synchronization the chaos of a Lorenz system, some parameters and states of the Lorenz system are replaced by chaotic signals.

$$\begin{cases} \dot{x}_1 = -\sigma(f - y_1) \\ \dot{y}_1 = rx_1 - y_1 - x_1 z_1 \\ \dot{z}_1 = x_1 y_1 - bz_1 \end{cases} \tag{4.3}$$

where σ =10, r =28, b =8/3, and the initial conditions are $x_1(0)$ = 0.001, $y_1(0)$ = 0.002, $z_1(0)$ = 0. The chaos excited Lorenz system is:

$$\begin{cases} \dot{x}_2 = -\sigma'(t)(f - y_2) \\ \dot{y}_2 = r'(t)x_2 - y_2 - x_2 z_2 \\ \dot{z}_2 = x_2 y_2 - b'(t)z_2 \end{cases} \tag{4.4}$$

where the initial condition is $x_2(0)$ = 0.002, $y_2(0)$ = 0.003, $z_2(0)$ = 0.001, and σ', r', b' are the parameters excited by chaotic signals. We define $e_1 = x_2 - x_1$, $e_2 = y_2 - y_1, e_3 = z_2 - z_1$.

For $f = kx_2, \sigma'(t) = \sigma, r'(t) = r, b'(t) = b$, with $k = 1$, two systems are synchronized , the time histories and the phase portrait are shown in Fig. 4.5-4.6.

For Eqs. (4.3) Eqs.(4.4) where the initial conditions are $x_2(0)$ = 0.002, $y_2(0)$ = 0.003, $z_2(0)$ = 0.001, and σ', r', b' are the parameters replaced , f is the state replaced.

For $f = kx_2, \sigma'(t) = \sigma, r'(t) = r, b'(t) = b$, with $k = 10$ two systems are synchronized, the time histories and the phase portrait is shown in Fig. 4.7-4.8

. For $f(x) = ky_2, \sigma'(t) = \sigma, r'(t) = r, b'(t) = b$, with $k = 1$ two systems are synchronized, the time histories and the phase portrait are shown in Fig. 4.9-4.10.

For $f(x) = ky_2, \sigma'(t) = \sigma, r'(t) = r, b'(t) = b$, with $k = 10$ two systems are synchronized, the time histories and the phase portrait are shown in Fig. 4.11-4.12.

If the chaos excited Lorenz systems becomes:

$$\begin{cases}\dot{x}_1 = -\sigma'(x_1 - y_1) \\ \dot{y}_1 = r' f_1 - y_1 - f_1 z_1 \\ \dot{z}_1 = x_1 y_1 - b'(t) z_1\end{cases} \tag{4.5}$$

$$\begin{cases}\dot{x}_2 = -\sigma'(t)(x_2 - y_2) \\ \dot{y}_2 = r'(t) f_1 - y_2 - f_2 z_2 \\ \dot{z}_2 = x_2 y_2 - b'(t) z_2\end{cases} \tag{4.6}$$

where the initial conditions are $x_2(0) = 0.002$, $y_2(0) = 0.003$, $z_2(0) = 0$, and σ', r', b' are the parameters replaced, f_1, f_2 are the states replaced.

For $f_1 = x_2$, $\sigma'(t) = \sigma, r'(t) = k, b'(t) = b$, $f_2 = px_2$ with $k = 28, p = 0.85$ two systems are synchronized, the time histories and the phase portrait are shown in Fig. 4.13.- 4.14.

For $f_1 = x_2$, $\sigma'(t) = \sigma, r'(t) = k, b'(t) = b$, $f_2 = px_2$, with $k = 28, p = 1.6$ two systems are synchronized, the time histories and the phase portrait are shown in Fig. 4.15.- 4.16.

For $f_1 = y_2$, $\sigma'(t) = \sigma, r'(t) = k, b'(t) = b$, $f_2 = py_2$ with $k = 28, p = 1$ two systems are synchronized, the time histories and the phase portrait are shown in Fig. 4.17 - 4.18.

For $f_1 = z_2$, $\sigma'(t) = \sigma, r'(t) = k, b'(t) = b$, $f_2 = pz_2$ with $k = 28, p = 1$ two systems are synchronized, the time histories and the phase portrait are shown in Fig. 4.19 - 4.20.

If the chaos excited Lorenz systems becomes:

$$\begin{cases}\dot{x}_1 = -\sigma(x_1 - y_1) \\ \dot{y}_1 = r x_1 - y_1 - x_1 z_1 \\ \dot{z}_1 = f(x) y_1 - b z_1\end{cases} \tag{4.7}$$

$$\begin{cases}\dot{x}_2 = -\sigma'(t)(x_2 - y_2) \\ \dot{y}_2 = r'(t) x_2 - y_2 - x_2 z_2 \\ \dot{z}_2 = f(x) y_2 - b'(t) z_2\end{cases} \tag{4.8}$$

For $\sigma'(t) = \sigma(\mathrm{t})$, $r'(t) = r(t), b'(t) = b$, $f = px_2$, with $p = 2$

For $r'(t) = px_2 + qy_2$, with $p = 0.1$, $q = 20$ two systems are synchronized the time histories and the phase portrait are shown in Fig. 4.21-4.22.

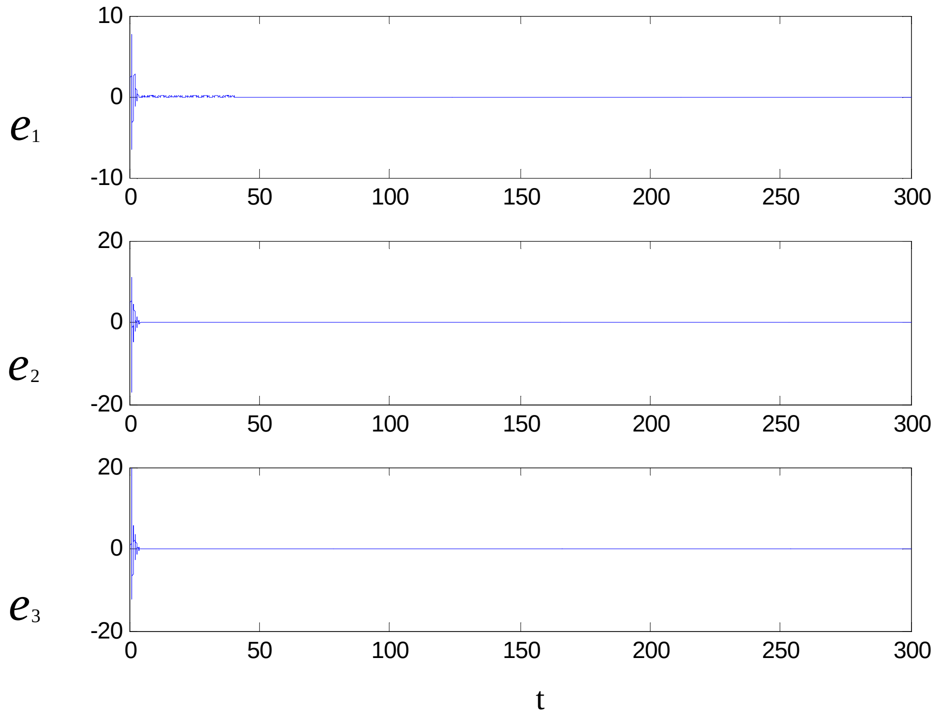

Fig.4. 1 Time histories of e_1, e_2, e_3, $\sigma'(t)=\sigma, r'(t)=r(t), b'(t)=|10\sin(t+0.5)|$

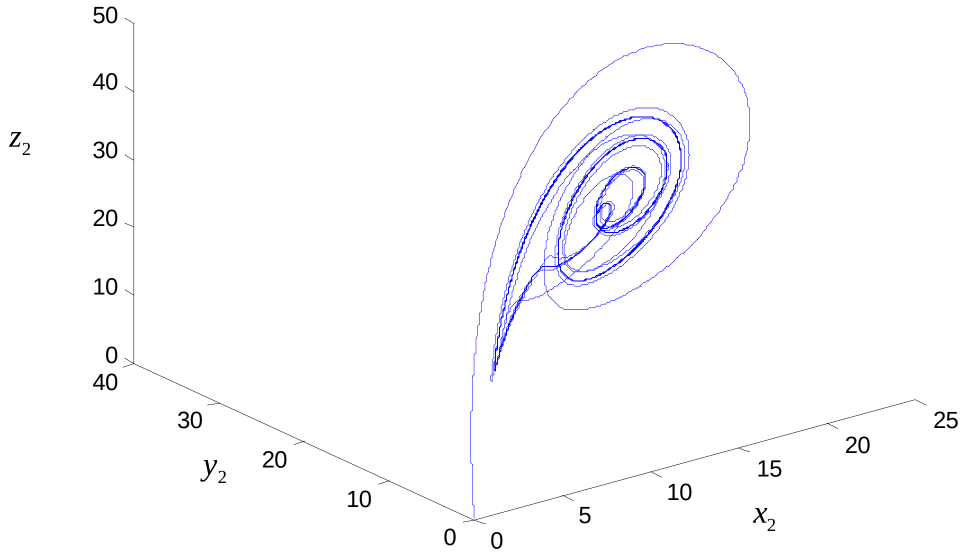

Fig.4. 2 Phase portrait of x_2, y_2, z_2 for $\sigma'(t)=\sigma, r'(t)=r(t), b'(t)=|10\sin(t+0.5)|$

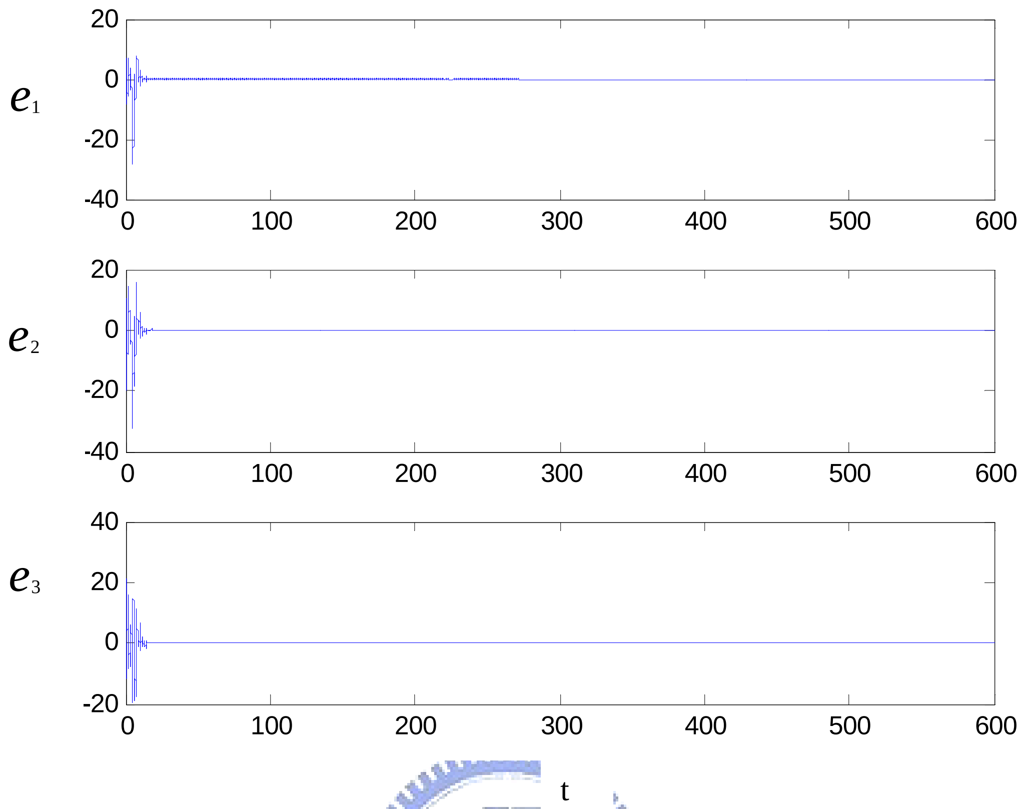

Fig.4. 3 Time histories of $e_1, e_2, e_3, \sigma'(t) = \sigma, r'(t) = r(t), b'(t) = |5\sin(5t + 0.1)|$

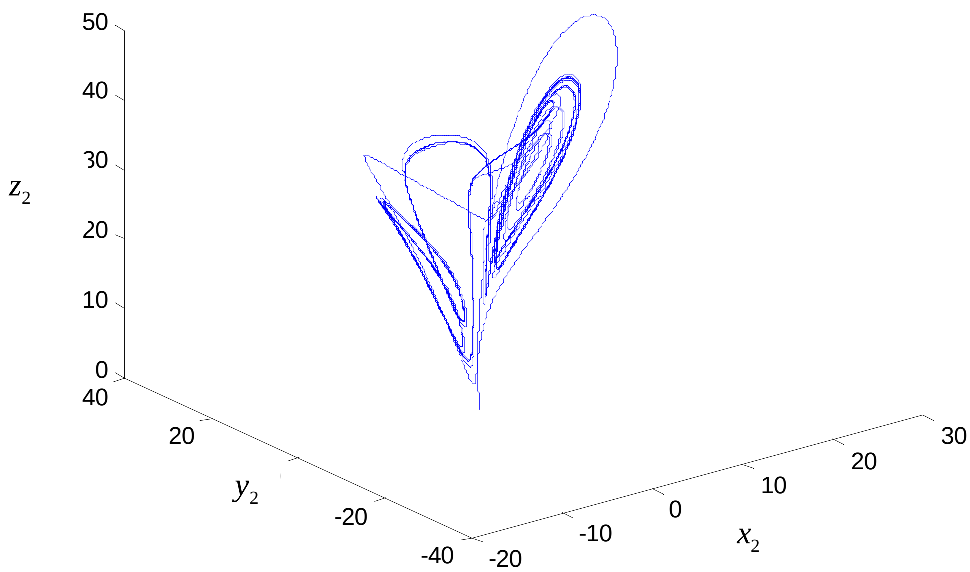

Fig.4. 4 Phase portrait of x_2, y_2, z_2 for $\sigma'(t) = \sigma, r'(t) = r(t), b'(t) = |5\sin(5t + 0.1)|$

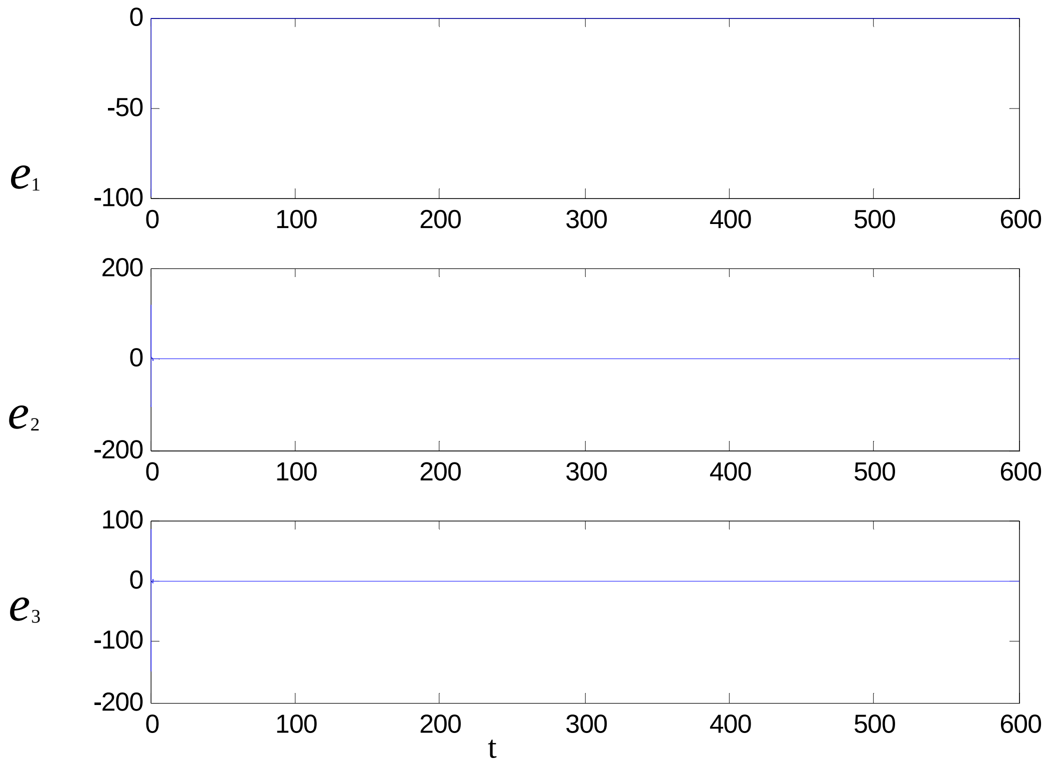

Fig.4. 5 Time histories of e_1, e_2, e_3, $f = x_2$, $\sigma'(t) = \sigma, r'(t) = r, b'(t) = b$.

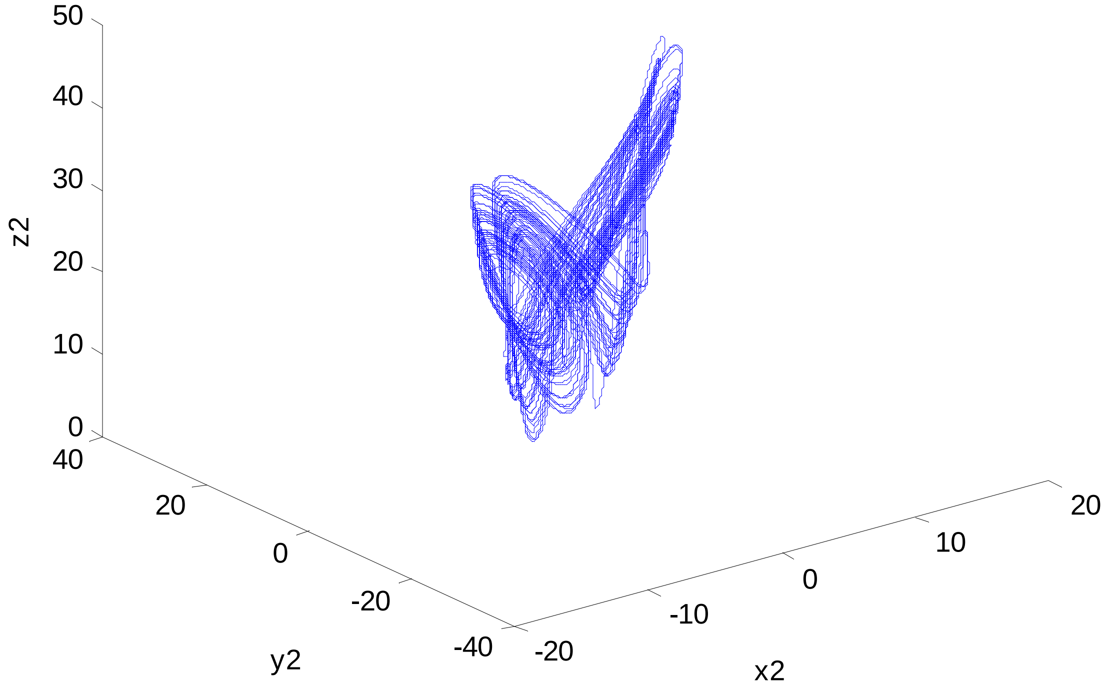

Fig.4. 6 Phase portrait of x_2, y_2, z_2 for $f = x_2$, $\sigma'(t) = \sigma, r'(t) = r, b'(t) = b$.

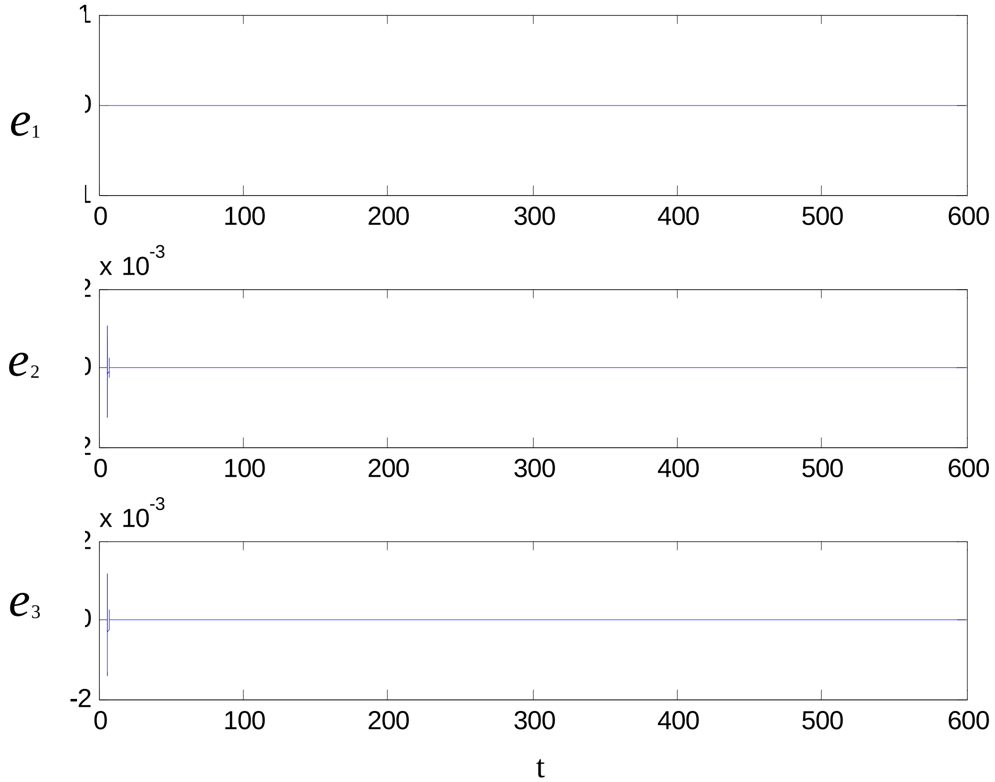

Fig.4. 7 Time histories of e_1, e_2, e_3, $f = 10x_2$, $\sigma'(t) = \sigma, r'(t) = r, b'(t) = b$.

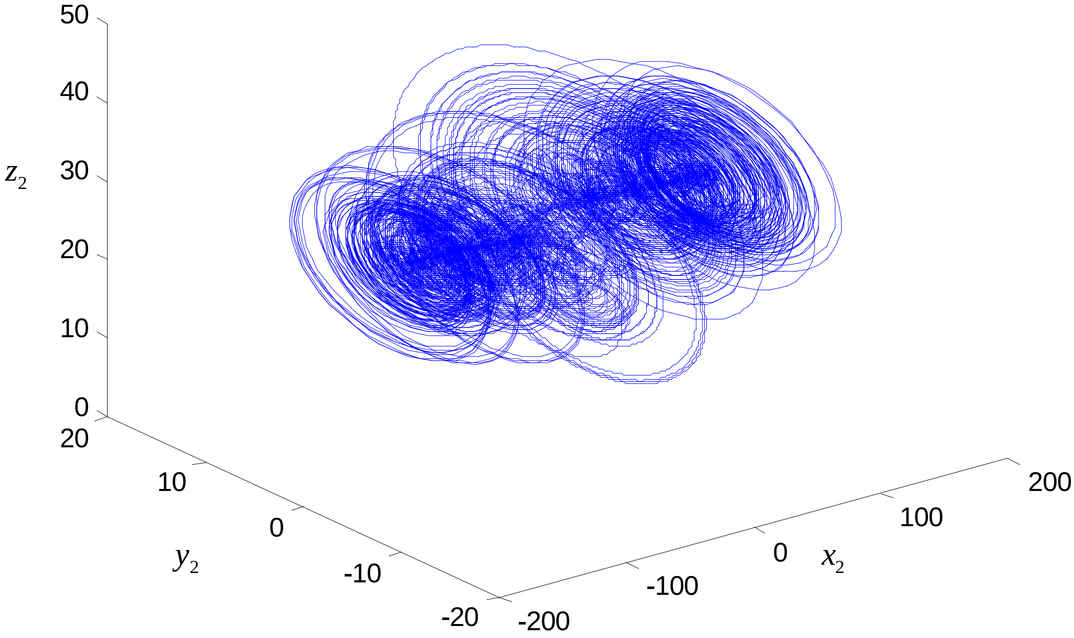

Fig.4. 8 Phase portrait of x_2, y_2, z_2 for $f = 10x_2$, $\sigma'(t) = \sigma, r'(t) = r, b'(t) = b$.

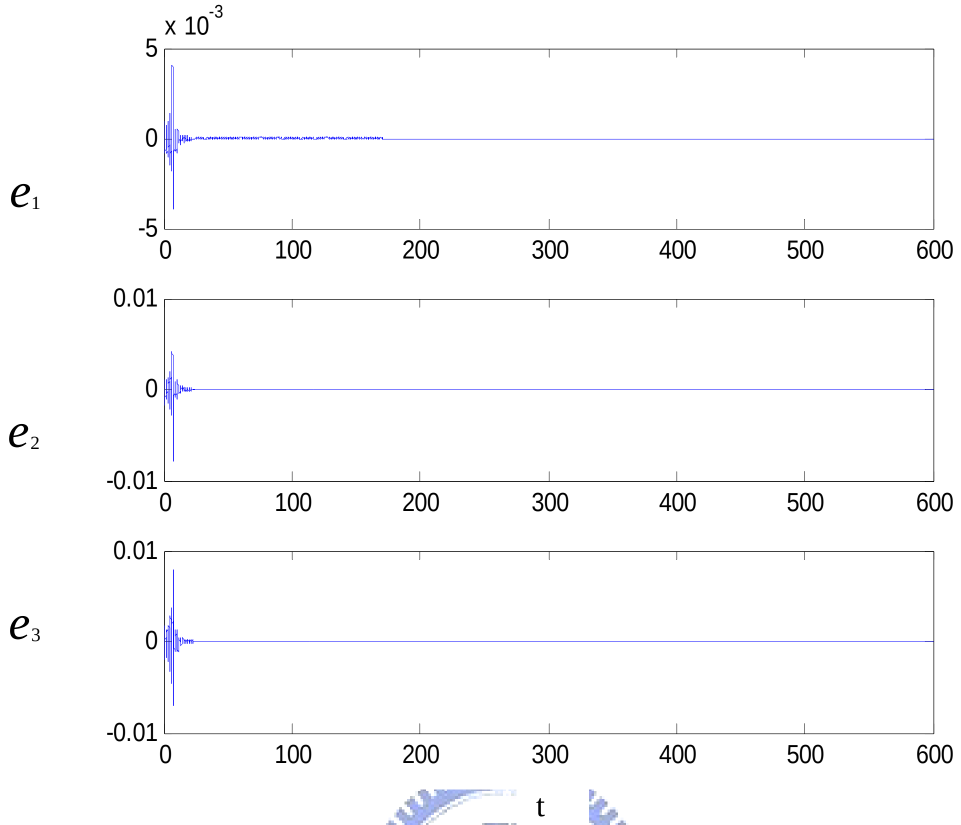

Fig.4. 9Time histories of e_1, e_2, e_3, $f(x) = y_2$, $\sigma'(t) = \sigma, r'(t) = r, b'(t) = b$.

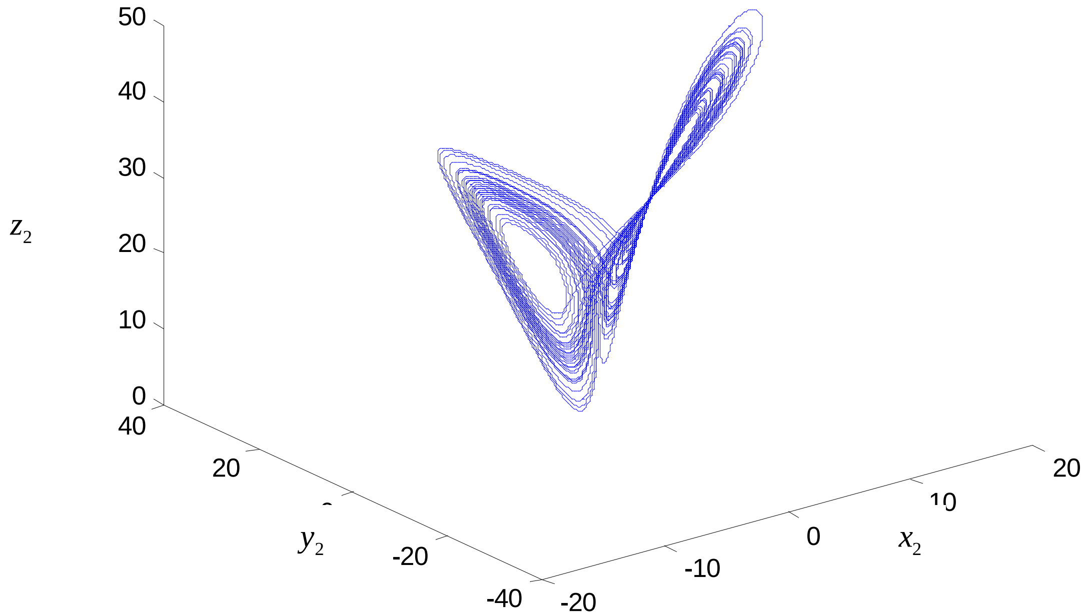

Fig.4. 10 Phase portrait of x_2, y_2, z_2 for $f(x) = y_2$, $\sigma'(t) = \sigma, r'(t) = r, b'(t) = b$.

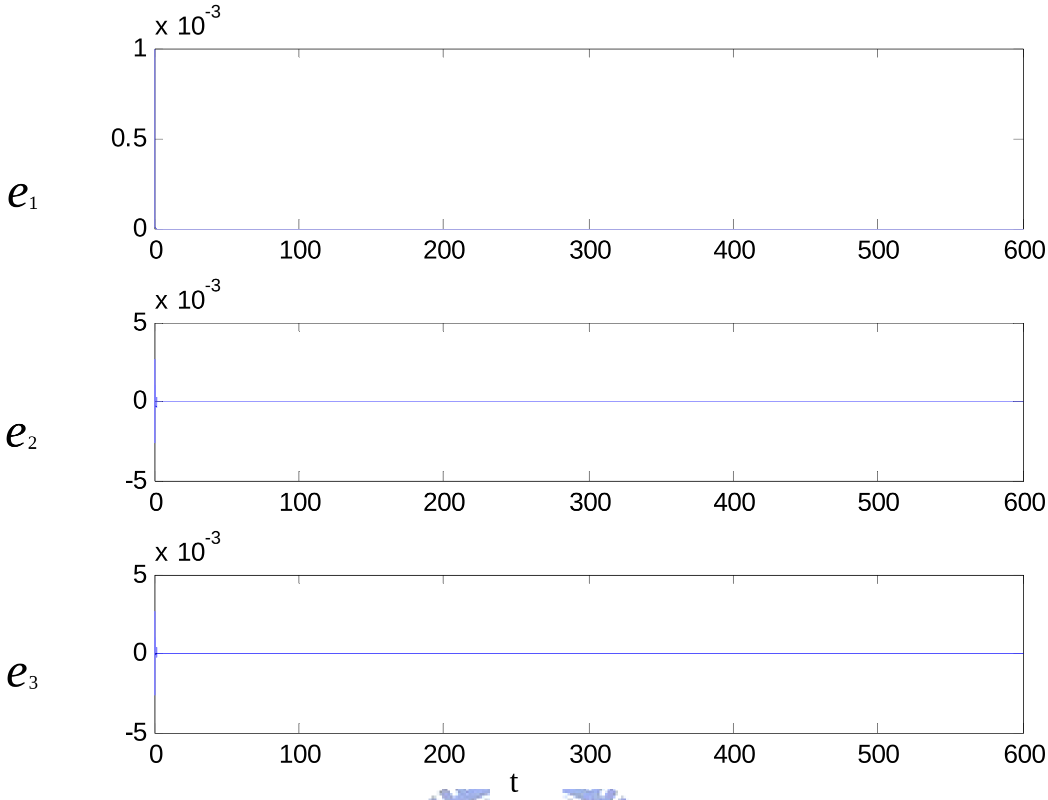

Fig.4. 11Time histories of e_1, e_2, e_3, $f = 10y_2$, $\sigma'(t) = \sigma, r'(t) = r, b'(t) = b$.

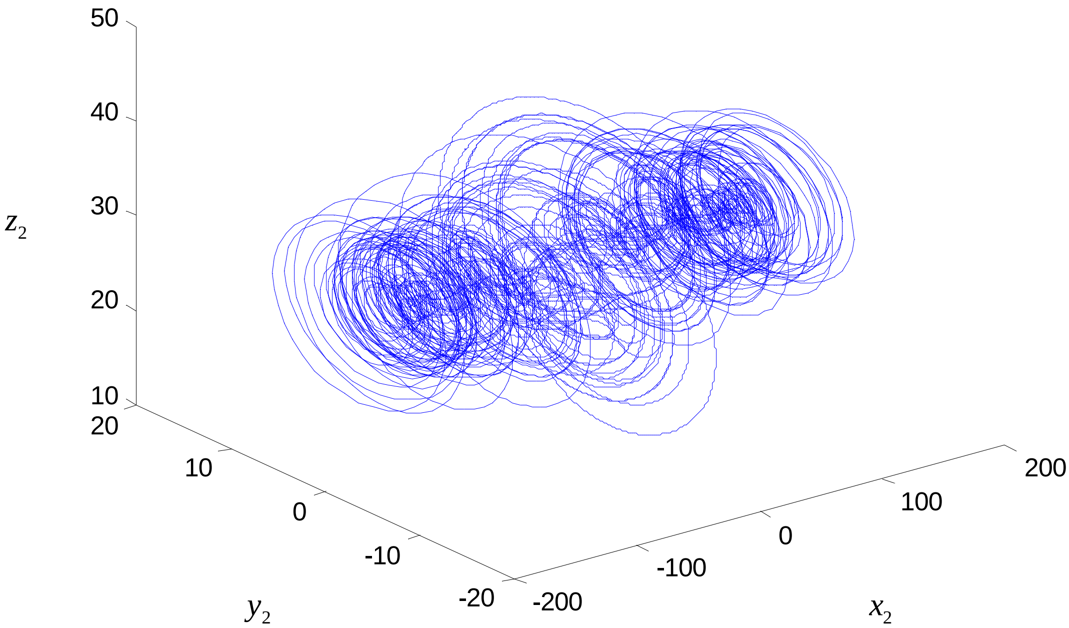

Fig.4. 12 Phase portrait of x_2, y_2, z_2 for $f = 10y_2$, x_2 $) = \sigma, r'(t) = r, b'(t) = b$.

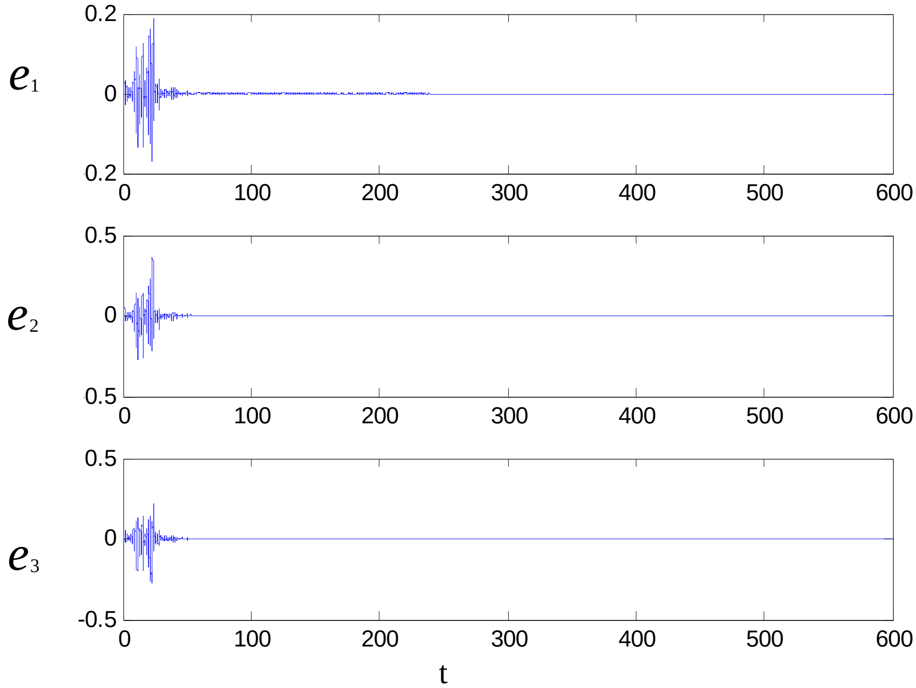

Fig.4. 13 Time histories for e_1, e_2, e_3 ， $f_1 = x_2$， $\sigma'(t) = \sigma, r'(t) = 28, b'(t) = b$， $f_2 = 0.85x_2$.

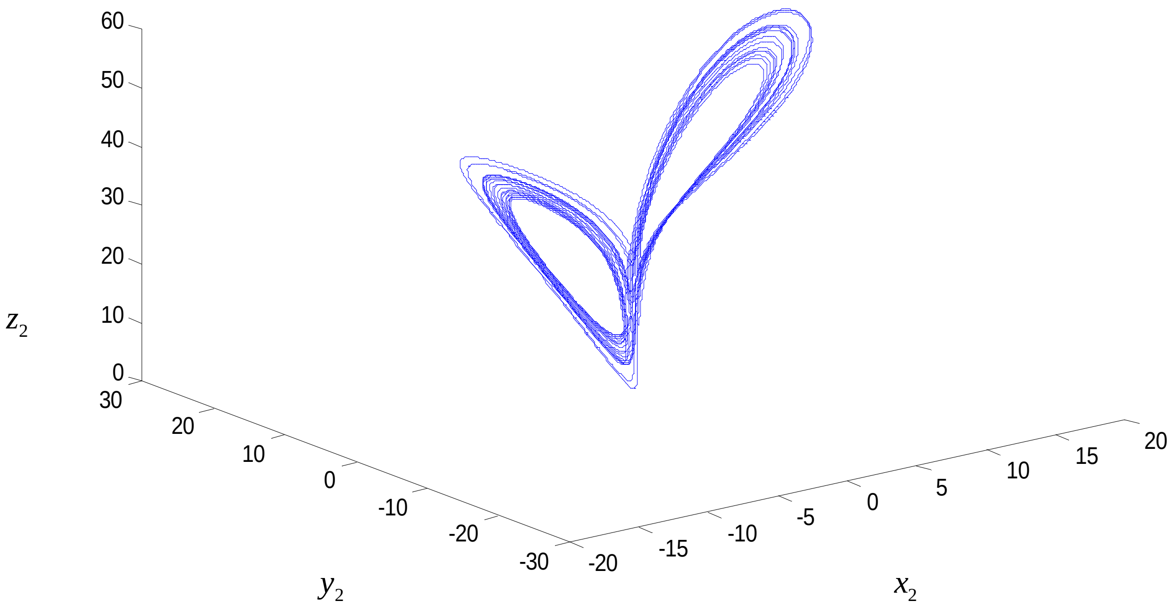

Fig.4. 14 Phase portrait of x_2, y_2, z_2 for $f_1 = x_2$， $\sigma'(t) = \sigma, r'(t) = 28, b'(t) = b$， $f_2 = 0.85x_2$.

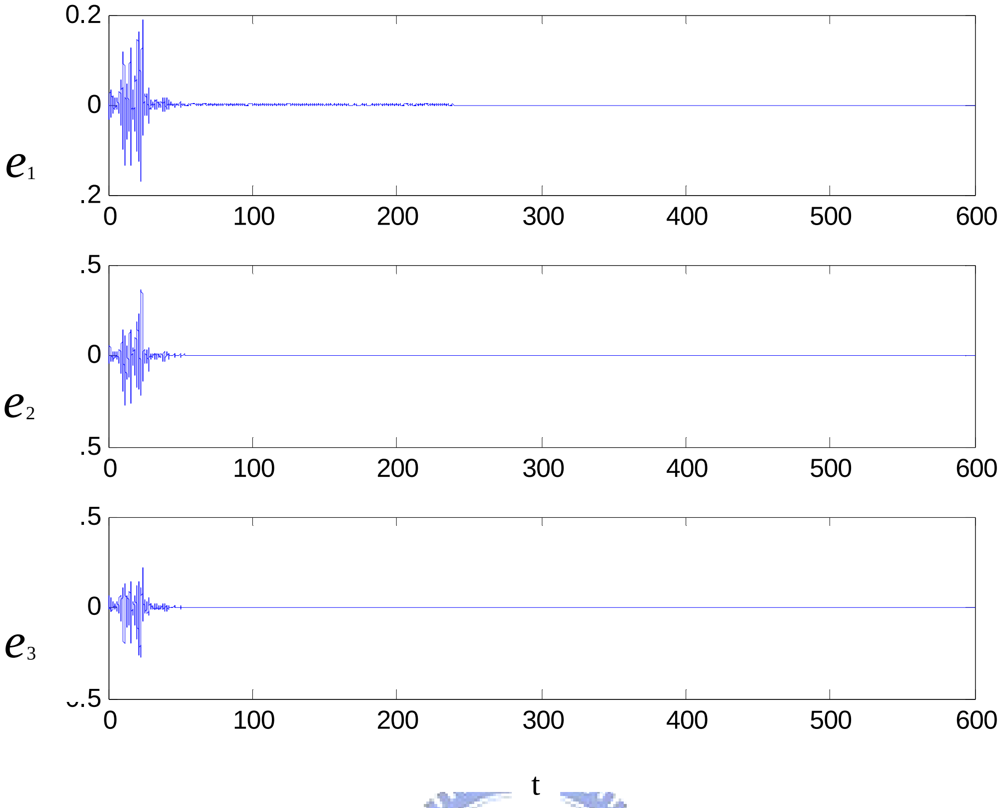

Fig.4. 15 Time histories of e_1, e_2, e_3 , $f_1 = x_2$, $\sigma'(t) = \sigma, r'(t) = 28, b'(t) = b$, $f_2 = 1.6x_2$.

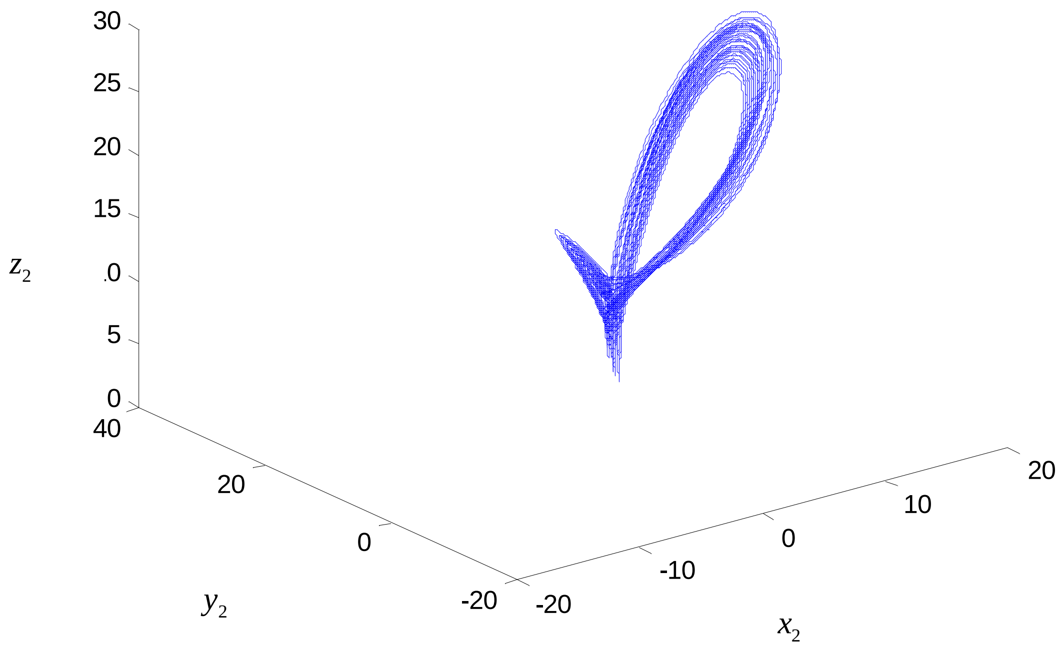

Fig.4. 16 Phase portrait of x_2, y_2, z_2 for $f_1 = x_2$, $\sigma'(t) = \sigma, r'(t) = 28, b'(t) = b$, $f_2 = 1.6x_2$.

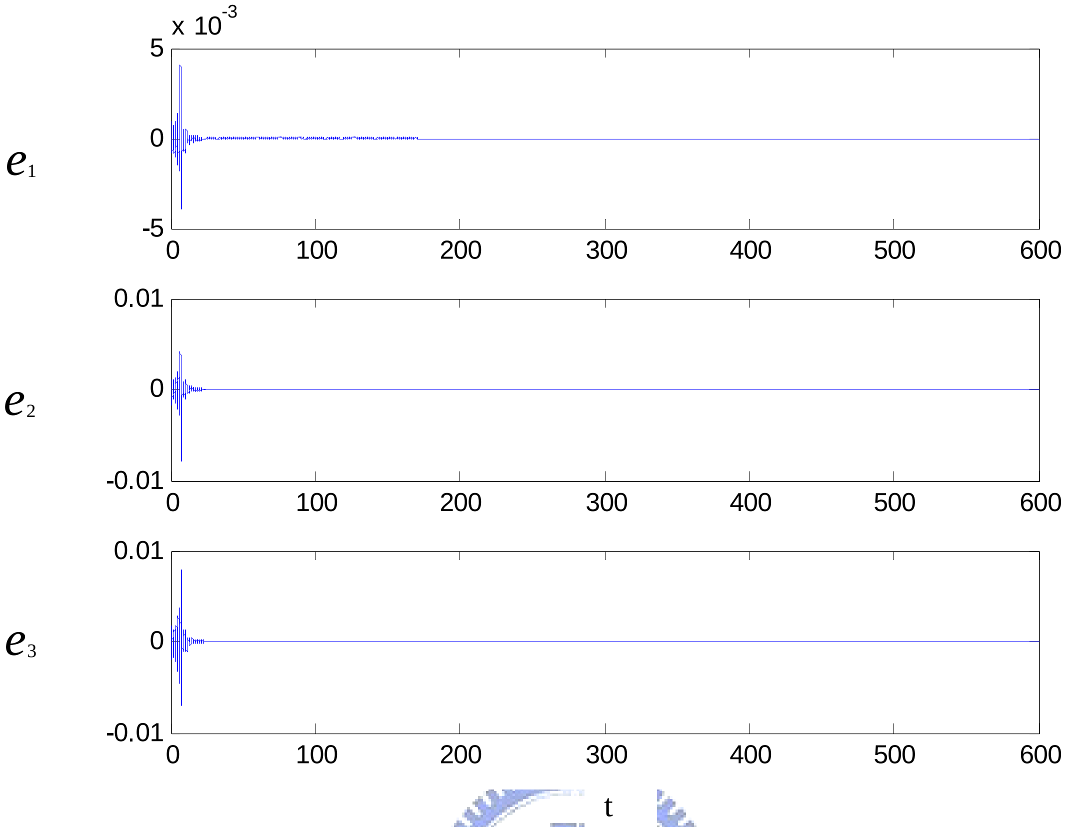

Fig.4. 17 Time histories of e_1, e_2, e_3 , $f_1 = y_2$, $\sigma'(t) = \sigma, r'(t) = 28, b'(t) = b$, $f_2 = y_2$.

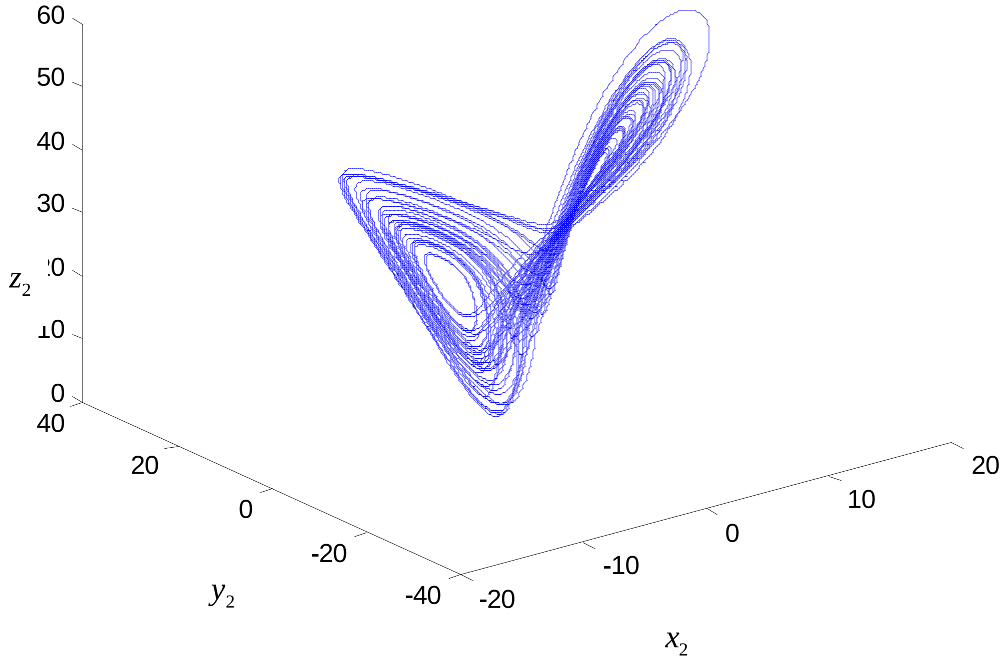

Fig.4. 18 Phase portrait of x_2, y_2, z_2 for $f_1 = y_2$, $\sigma'(t) = \sigma, r'(t) = 28, b'(t) = b$, $f_2 = y_2$.

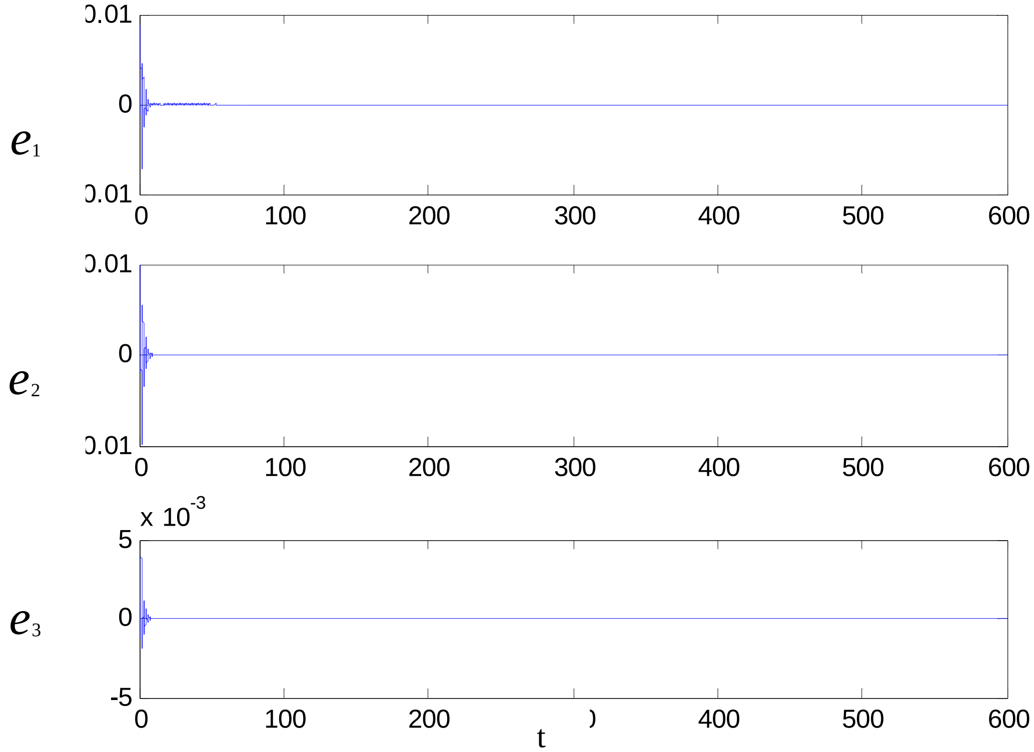

Fig.4. 19 Time histories of e_1, e_2, e_3 , $f_1 = z_2$, $\sigma'(t) = \sigma, r'(t) = 28, b'(t) = b$, $f_2 = z_2$.

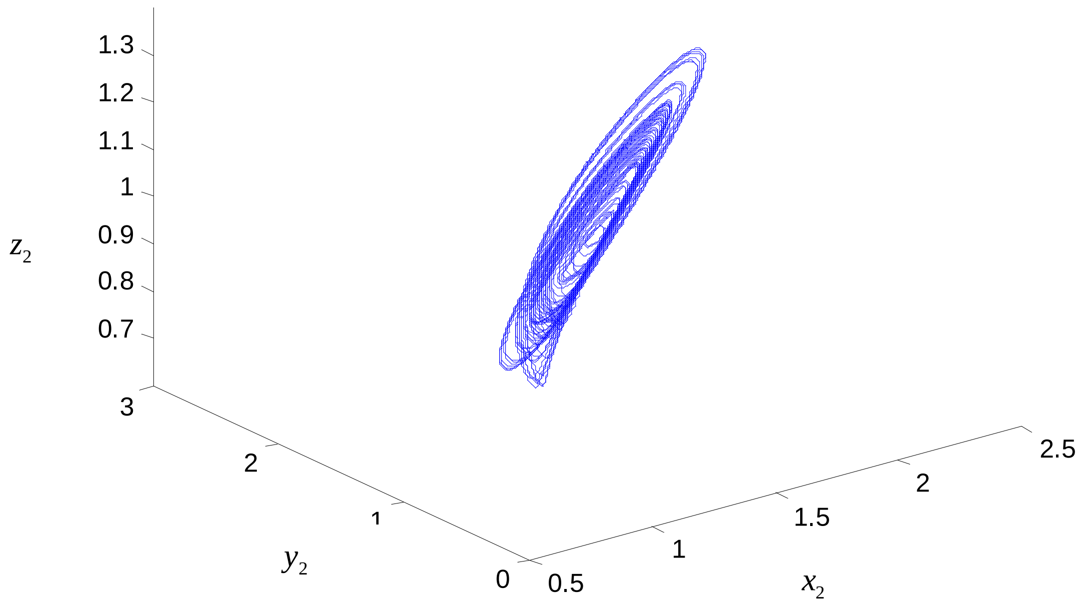

Fig.4. 20 Phase portrait of x_2, y_2, z_2 for $f_1 = x_2, \sigma'(t) = \sigma, r'(t) = 28, b'(t) = b$, $f_2 = x_2$.

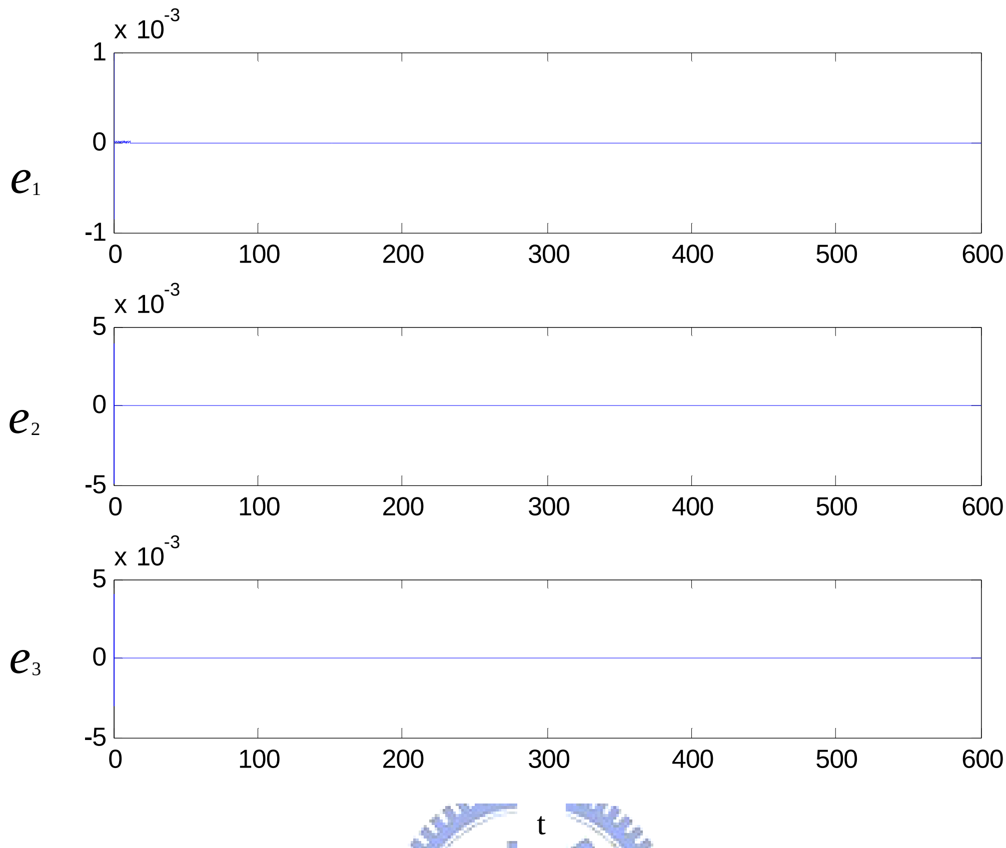

Fig.4. 21 Time histories of $e_1, e_2, e_3, r'(t) = r(t) = 0.1x_2 + 20y_2, \sigma'(t) = \sigma, b'(t) = b$.

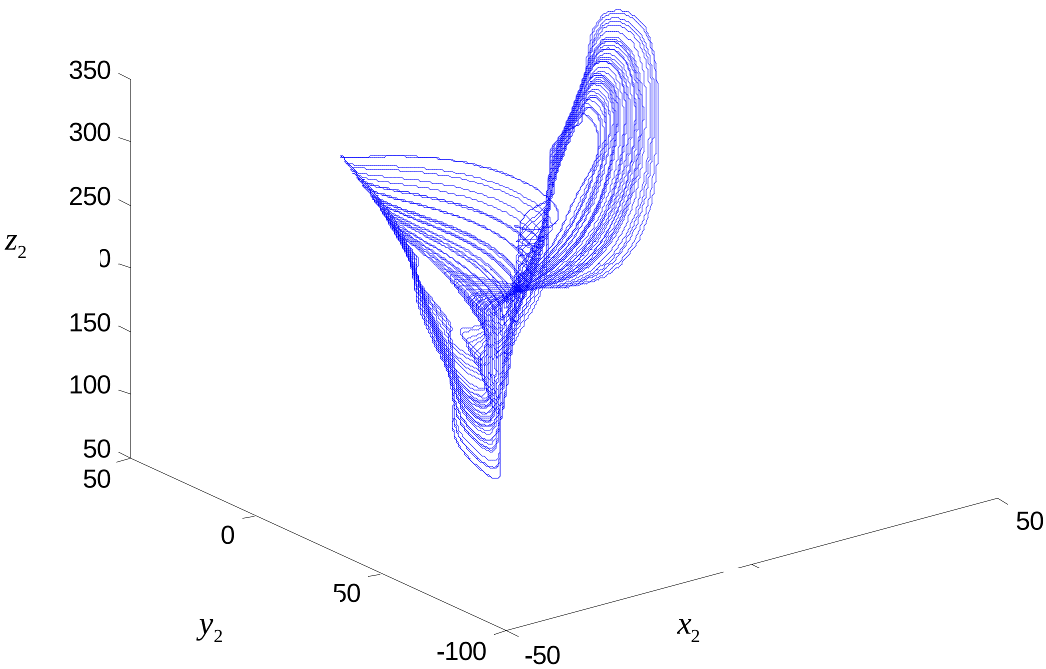

Fig.4. 22 Phase portrait of $x_2, y_2, z_2, r'(t) = r(t) = 0.1x_2 + 20y_2, \sigma'(t) = \sigma, b'(t) = b$.

Chapter 5

Uncoupled Chaos Synchronization of Two Lorenz Systems by Replacing of Parameter by Chaotic and Regular Function

In order to obtain uncoupled chaos synchronization of two Lorenz systems, the corresponding parameters are replaced by a function of regular function of time and state of a third Lorenz system.

There are two Lorenz systems of which two corresponding parameters are replaced by a regular function of time. Two identical Lorenz systems to be synchronized are:

$$\begin{cases} \dot{x}_1 = -\sigma(x_1 - y_1) \\ \dot{y}_1 = rx_1 - y_1 - x_1 z_1 \\ \dot{z}_1 = x_1 y_1 - bz_1 \end{cases} \tag{5.1}$$

$$\begin{cases} \dot{x}_2 = -\sigma'(x_2 - y_2) \\ \dot{y}_2 = r'x_2 - y_2 - x_2 z_2 \\ \dot{z}_2 = x_2 y_2 - b'z_2 \end{cases} \tag{5.2}$$

where $\sigma = \sigma'$ =10, $r = r'$=28, $b = b'$=8/3, and the initial conditions are x_1(0)=0.001, y_1(0)=0.002, z_1(0)=0. x_2(0)=0.001, y_2(0) = 0.002, z_2(0) = 0.001, the third Lorenz system is:

$$\begin{cases} \dot{x}_3 = -\sigma(x_3 - y_3) \\ \dot{y}_3 = rx_3 - y_3 - x_3 z_3 \\ \dot{z}_3 = x_3 y_3 - bz_3 \end{cases} \tag{5.3}$$

with initial condition x_3(0)=0.001, y_3(0)=0.002, z_3(0)=0.001.

We define $e_1 = x_2 - x_1$, $e_2 = y_2 - y_1$, $e_3 = z_2 - z_1$.

(1) $r(t) = r'(t) = A\sin(\omega t + p)$

When A=25, ω =20, p=0.5 two system are synchronized. The time histories of e_1, e_2, e_3 and the phase portrait are shown in Fig. 5.1-5.2.

(2) $b'(t) = b(t) = Ax_3 \sin(\omega t)$

When A=0.5, ω=10 two systems are synchronized. The time histories of e_1, e_2, e_3 and the phase portrait are shown in Fig. 5.3-5.4.

(3) $b'(t) = b(t) = \left| kx_3 \sin(\omega t) + y_3 \right|$

When A=0.5, ω=10 two systems are synchronized. The time histories of e_1, e_2, e_3 and the phase portrait are shown in Fig. 5.5-5.6.

(4) $b(t) = b'(t) = A\sin(\omega \sin(\omega_1 t))$

When A=10, ω=0.5, ω_1 =20 two systems are synchronized. The time histories of e_1, e_2, e_3 and the phase portrait are shown in Fig. 5.7-5.8.

(5) $b(t) = b'(t) = A\sin(\omega + k\sin(\omega_1 t + p))$

When A= 2, ω=9.99, ω_1 =10, k=1, p=0.6 two system are synchronized.

The time histories of e_1, e_2, e_3 and the phase portrait are shown in Fig. 5.9-5.10.

(6) $\sigma(t) = \sigma'(t) = A\sin(\omega + k\sin(\omega_1 t + p))$

When A=17, ω=9.99, ω_1 =10, k=2, p=1.2 two system are synchronized.

The time histories of e_1, e_2, e_3 and the phase portrait are shown in Fig. 5.11-5.12.

(7) $b'(t) = ky_2 \sin(\omega + (\sin(\omega_1 t + p))$,

When k=32, ω=9.99, $\omega_1 = 10$,p=1.2 two system are synchronized. The time histories of e_1, e_2, e_3 and the phase portrait are shown in Fig. 5.13-5.14.

(8) $b = b'(t) = \left| A\sin(\omega t + p) / x_3 \right|$

When A=7, ω=5, $p = 0.1$ two system are synchronized.

The time histories of e_1, e_2, e_3 and the phase portrait are shown in Fig. 5.15-5.16.

When $b'(t) = \left| ky_2 \sin(\omega(\sin(\sin(\omega_1 t)))) \right|$, when k=10, ω=0.5, $\omega_1 = 1$ two system are synchronized. The time histories of e_1, e_2, e_3 and the phase portrait are shown in Fig. 5.17-5.18.

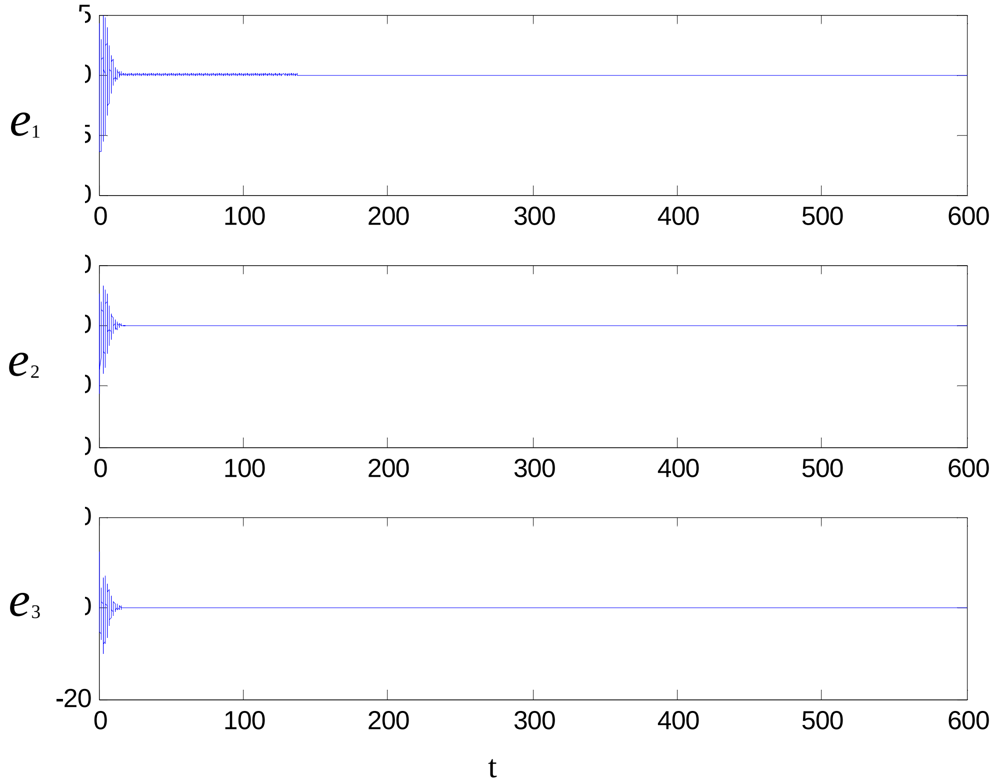

Fig.5. 1 Time histories of e_1, e_2, e_3 for $r(t) = r'(t) = 25\sin(20t + 0.5)$

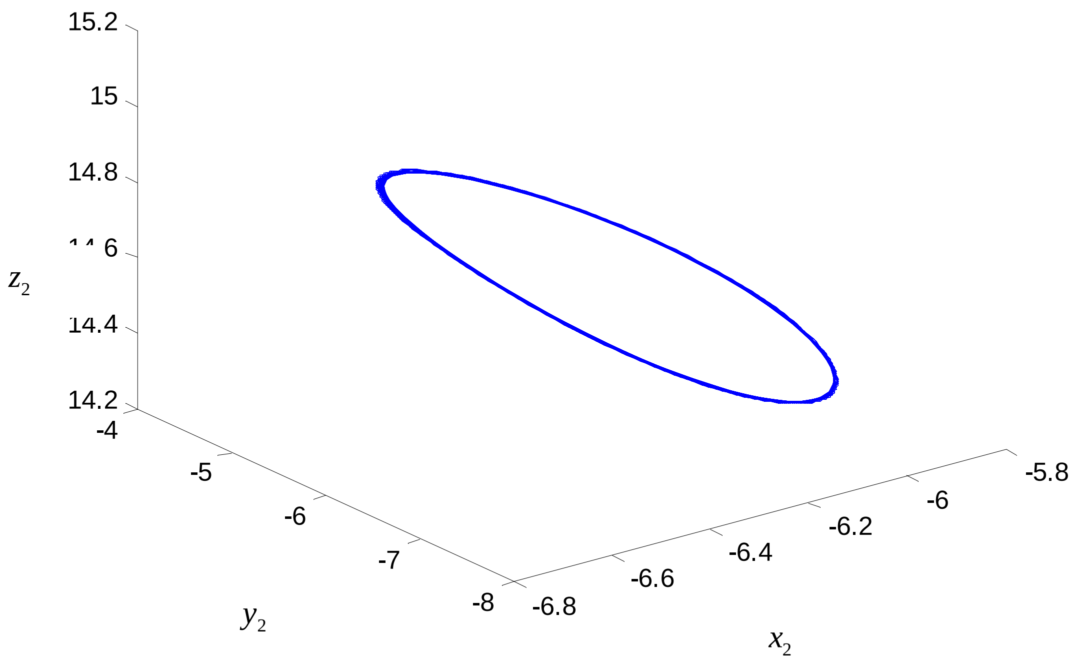

Fig.5. 2 Phase portrait of x_2, y_2, z_2 for $r(t) = r'(t) = 25\sin(20t + 0.5)$

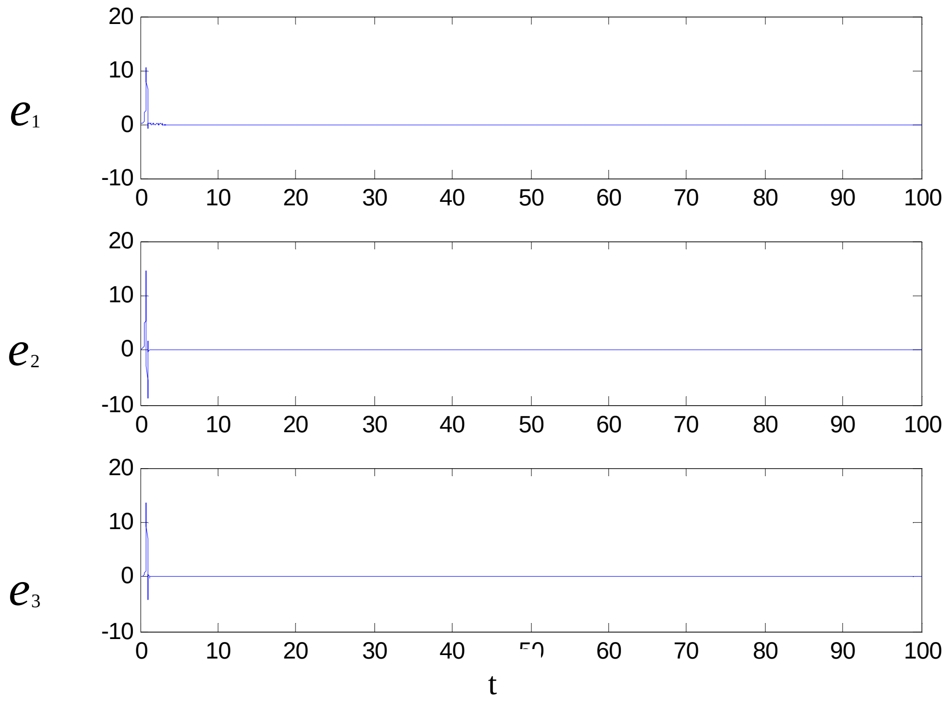

Fig.5. 3 Time histories of e_1, e_2, e_3 for $b'(t) = b(t) = 0.5\sin(10t)$

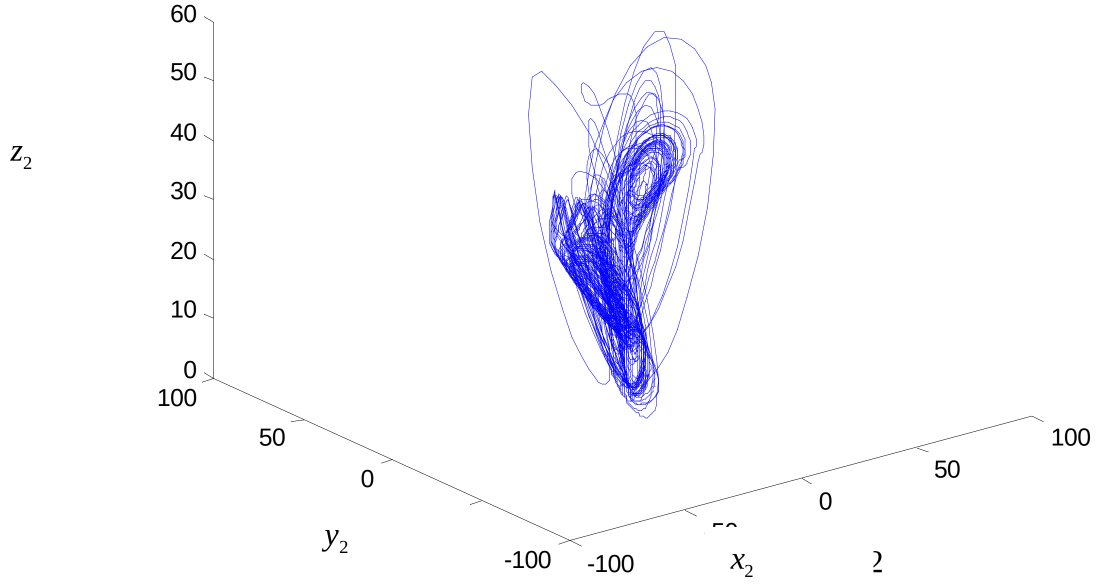

Fig.5. 4 Phase portrait of x_2, y_2, z_2 for $b'(t) = b(t) = 0.5\sin(10t)$

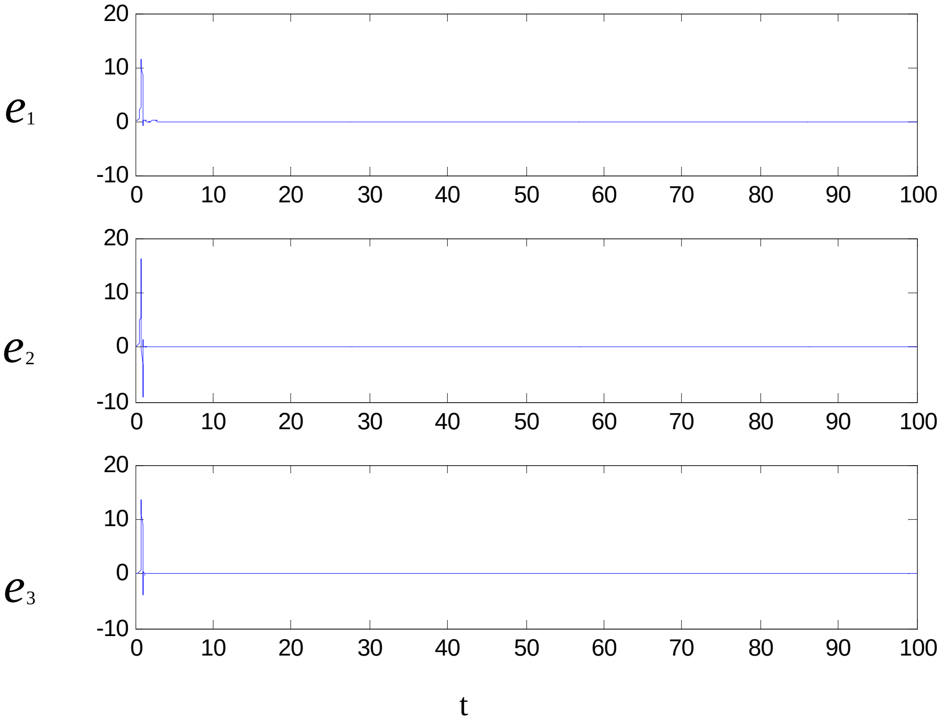

Fig.5. 5 Time histories of e_1, e_2, e_3 for $b'(t) = b(t) = |1/2 x_3 \sin(1/2t) + y_3|$.

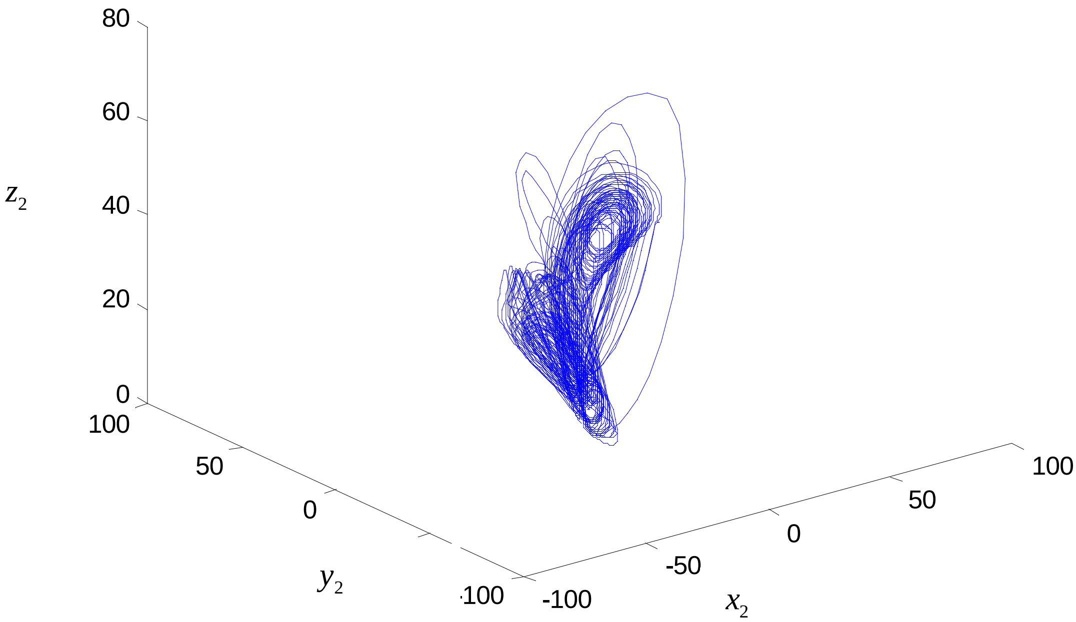

Fig.5. 6 Phase portrait of x_2, y_2, z_2 for $b'(t) = b(t) = |1/2 x_3 \sin(10t) + y_3|$.

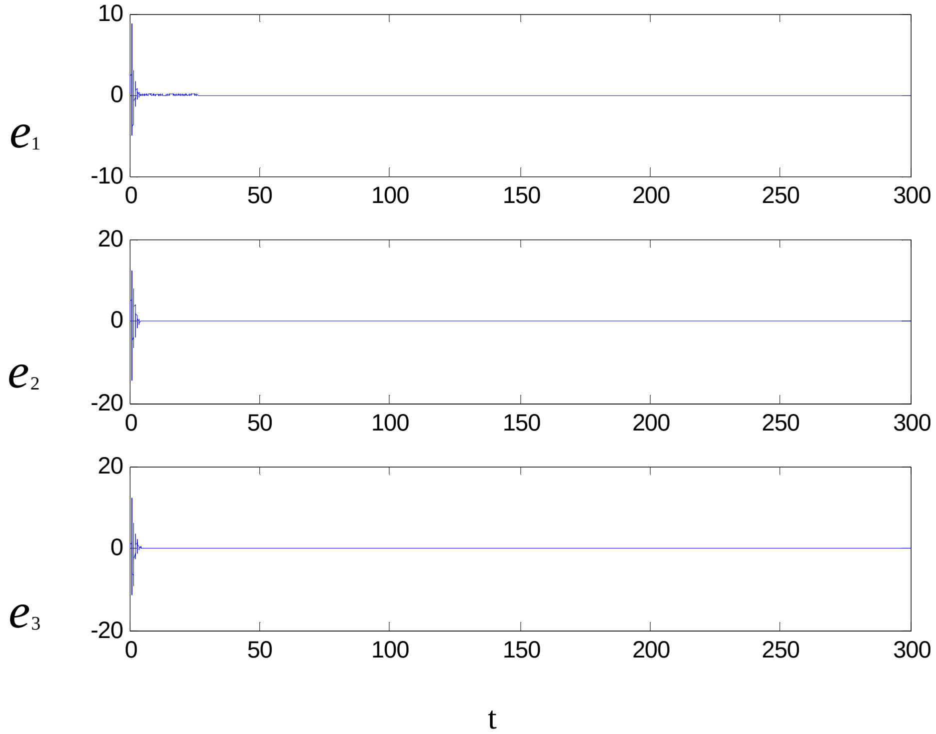

Fig.5. 7 Time histories of e_1, e_2, e_3 for $b'(t) = 10\sin(0.5\sin(20t))$.

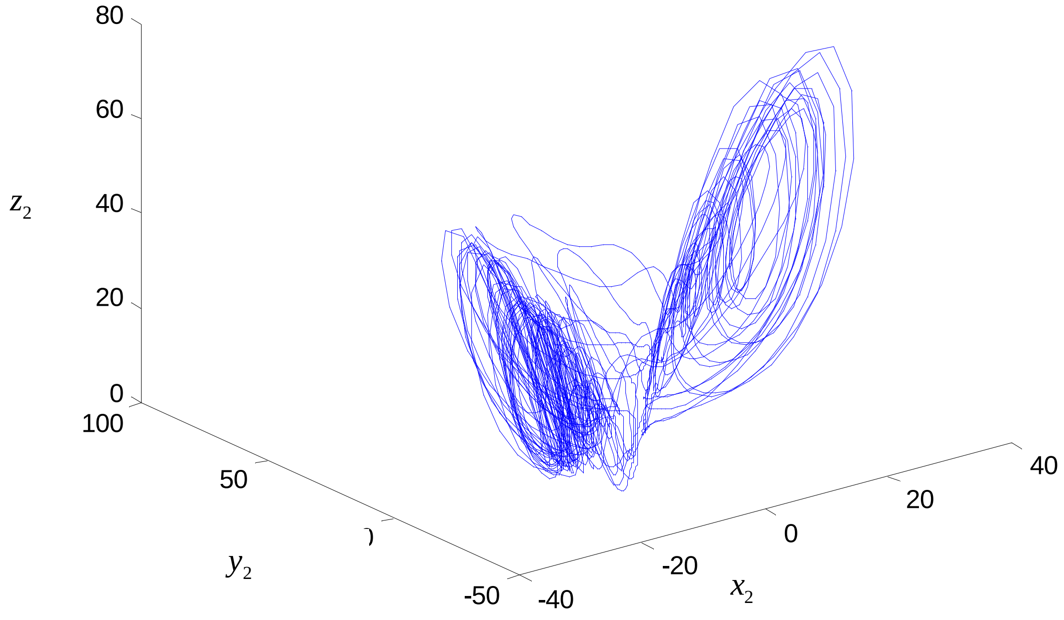

Fig.5. 8 Phase portrait of x_2, y_2, z_2 for $b'(t) = 10\sin(0.5\sin(20t))$.

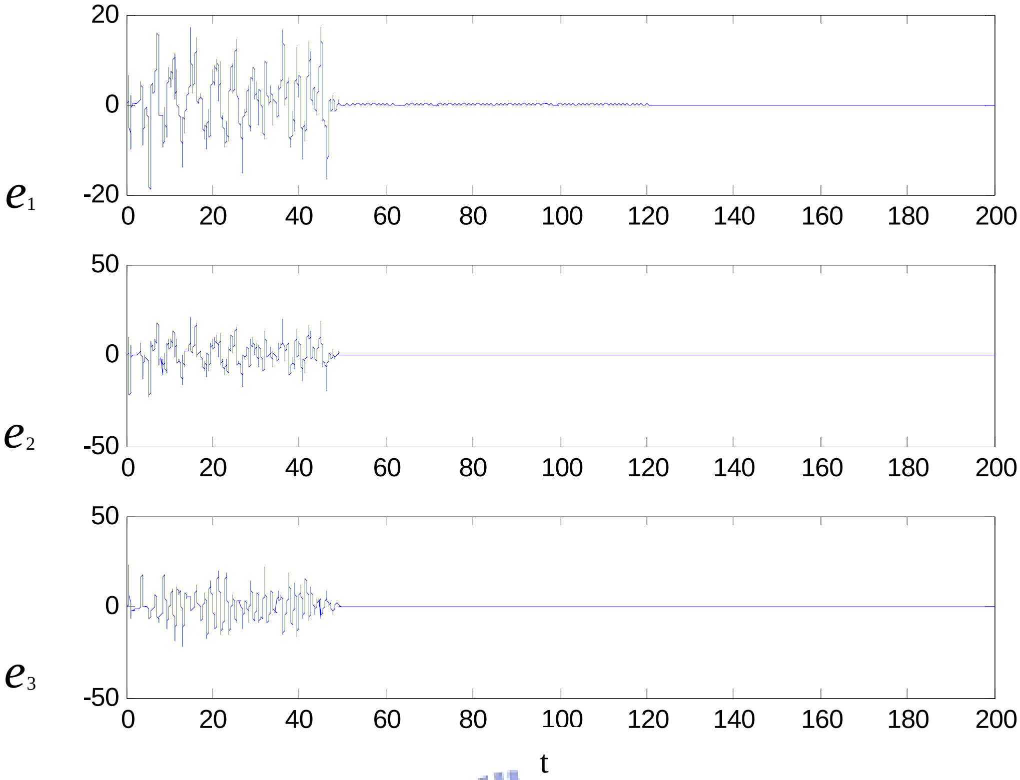

Fig.5. 9 Time histories of x_2, y_2, z_2 for $b'(t) = 2\sin(9.99 + \sin(10t + 0.6))$.

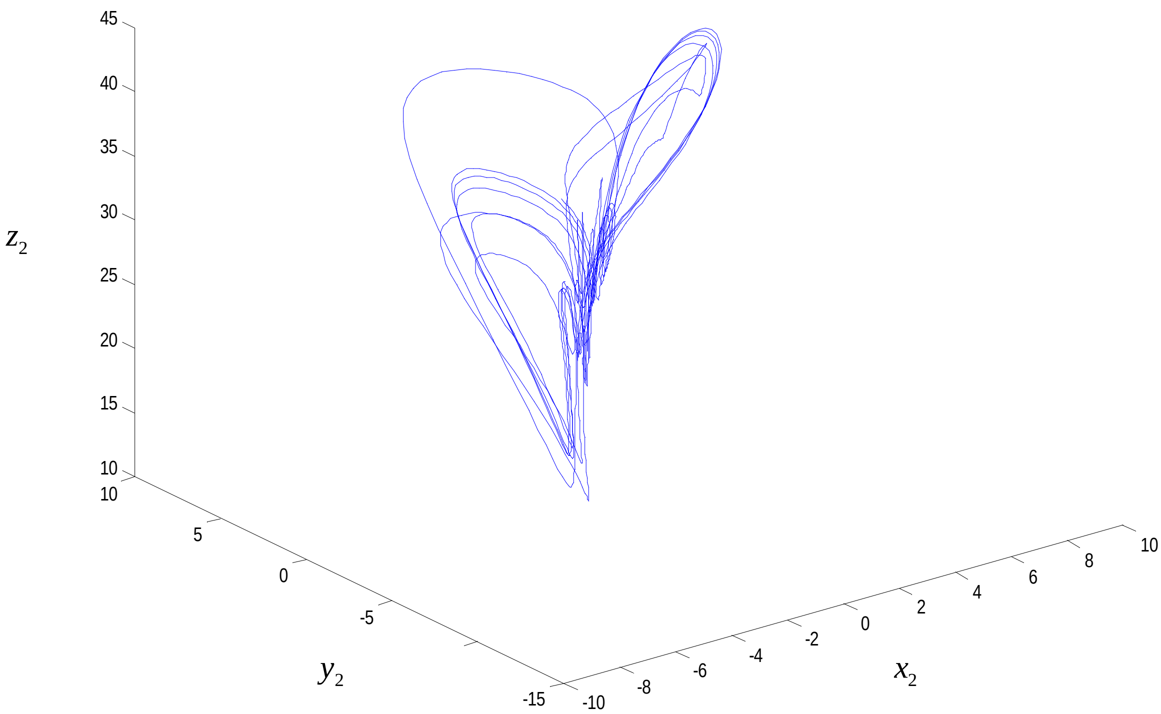

Fig.5. 10Phase portrait of x_2, y_2, z_2 for $b'(t) = 2\sin(9.99 + \sin(10t + 0.6))$.

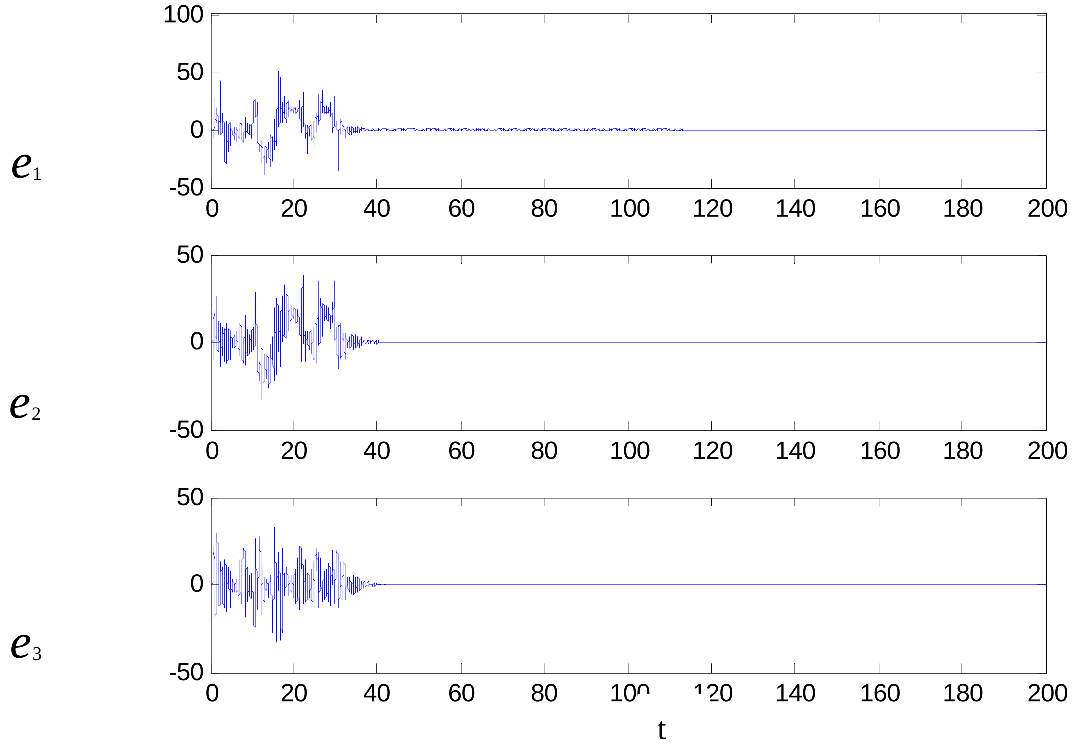

Fig.5. 11Time histories of x_2, y_2, z_2 when $\sigma'(t) = 17\sin(9.99 + 2\sin(10t + 1.2))$.

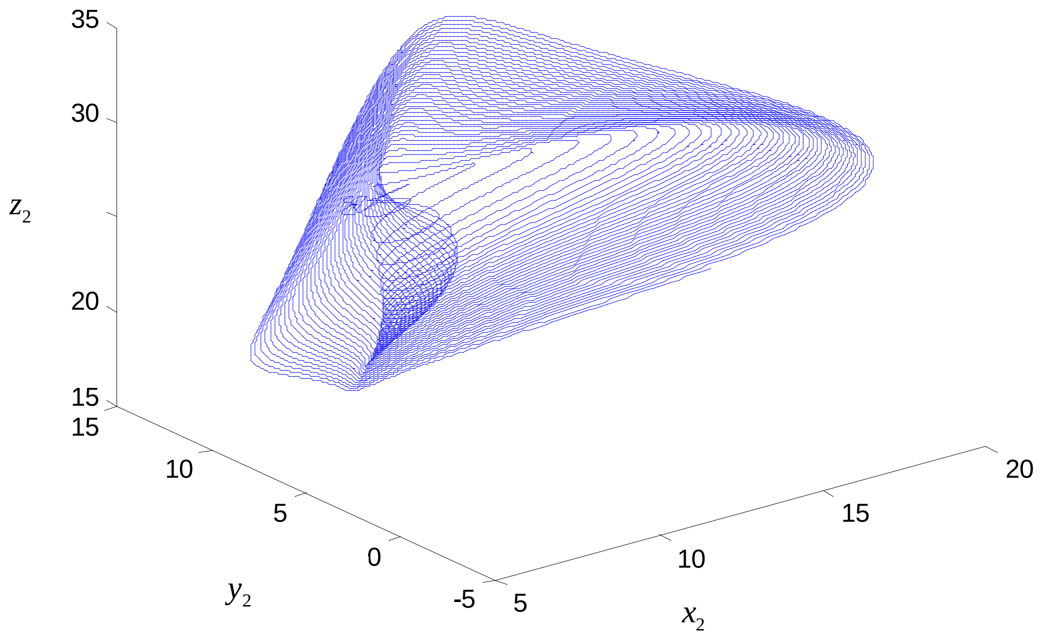

Fig.5. 12 Phase portrait of x_2, y_2, z_2 for $\sigma'(t) = 17\sin(9.99 + 2\sin(10t + 1.2))$.

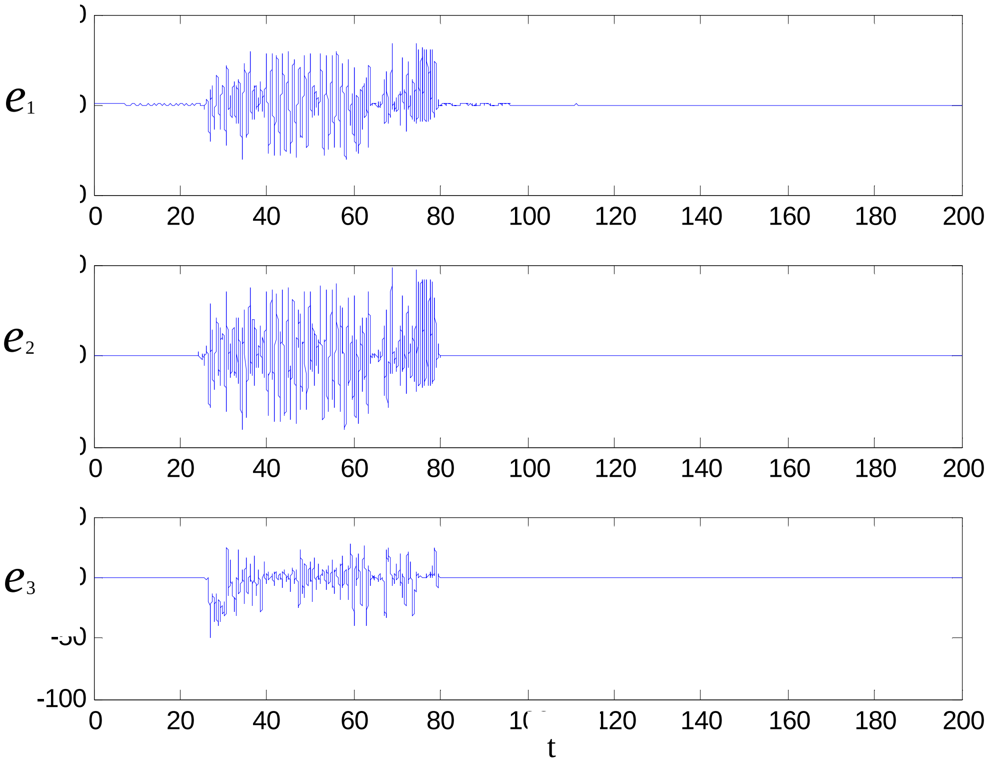

Fig.5. 13 Time histories of x_2, y_2, z_2 when $r(t) = r'(t) = 32\sin(9.99 + 2\sin(10t + 1.2))$.

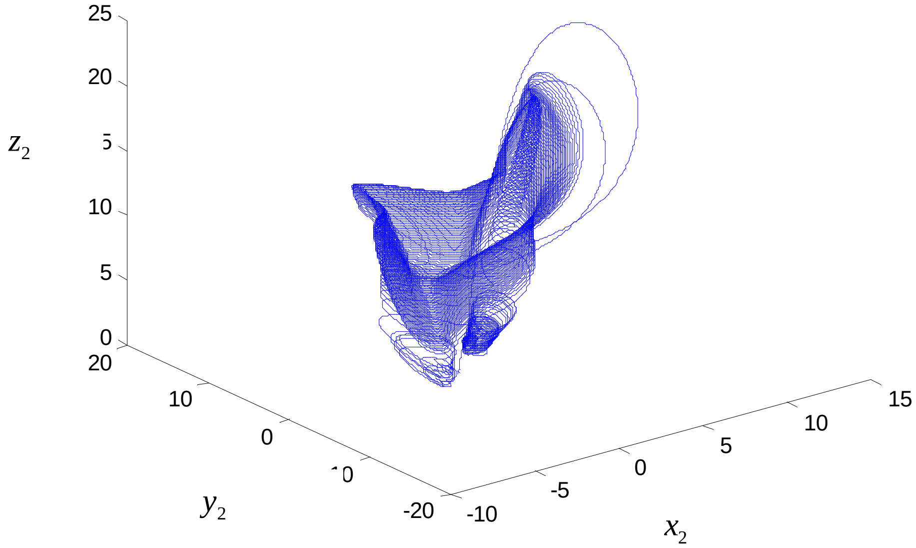

Fig.5. 14 Phase portrait of x_2, y_2, z_2 for $r(t) = r'(t) = 32\sin(9.99 + 2\sin(10t + 1.2))$

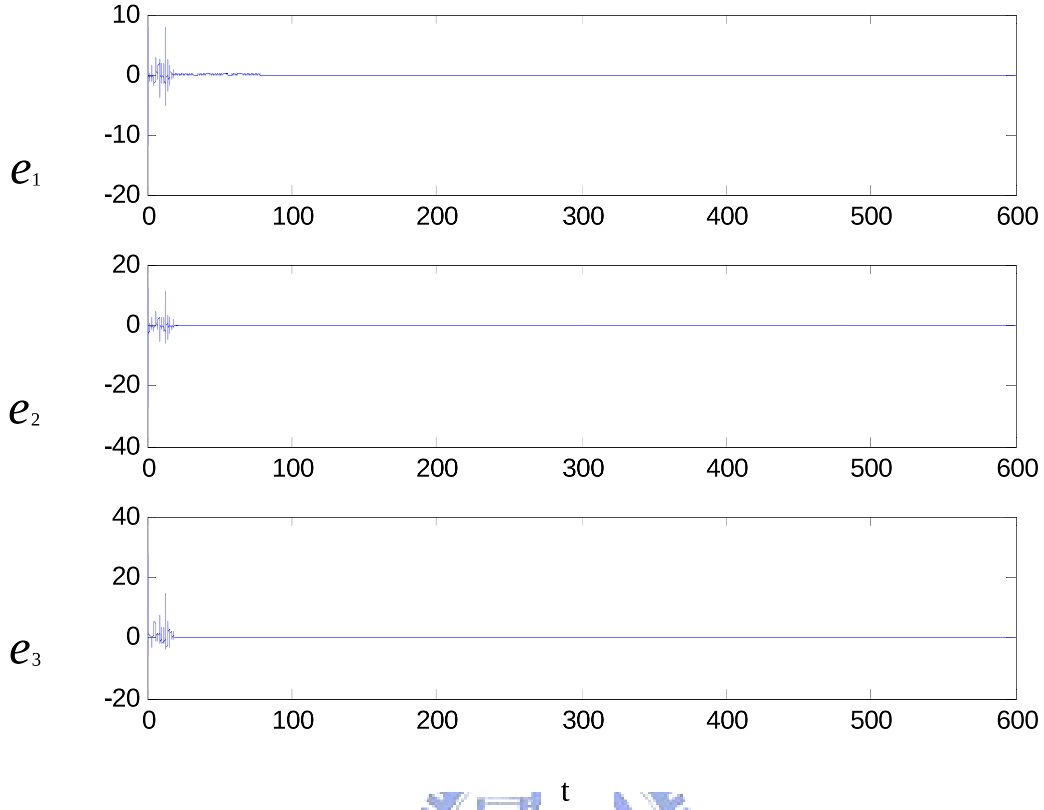

Fig.5. 15Time histories of x_2, y_2, z_2 when $b = b'(t) = |7\sin(5t + 0.1) / x_3|$.

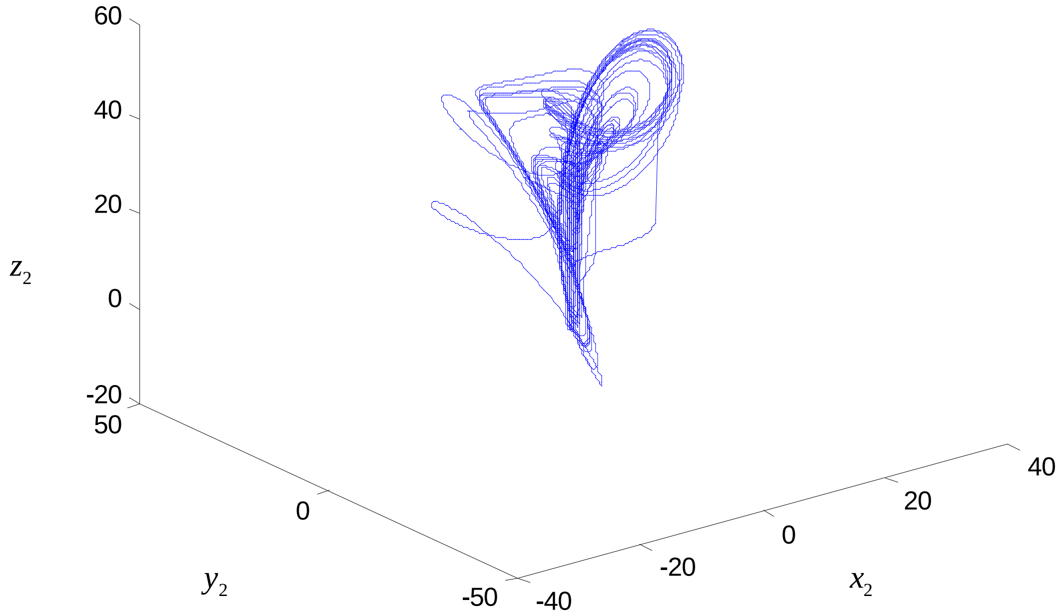

Fig.5. 16Phase portrait of x_2, y_2, z_2 for $b = b'(t) = |7\sin(5t + 0.1) / x_3|$.

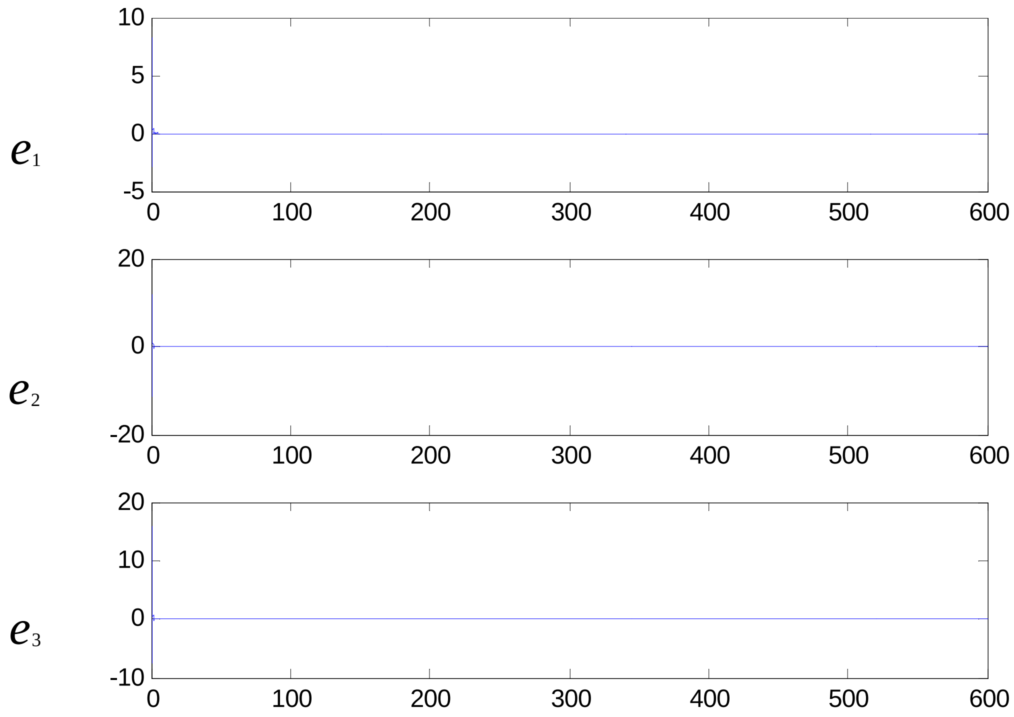

Fig.5. 17 Time histories of x_2, y_2, z_2 for $b'(t) = |10y_2 \sin(0.5(\sin(\sin(t))))|$

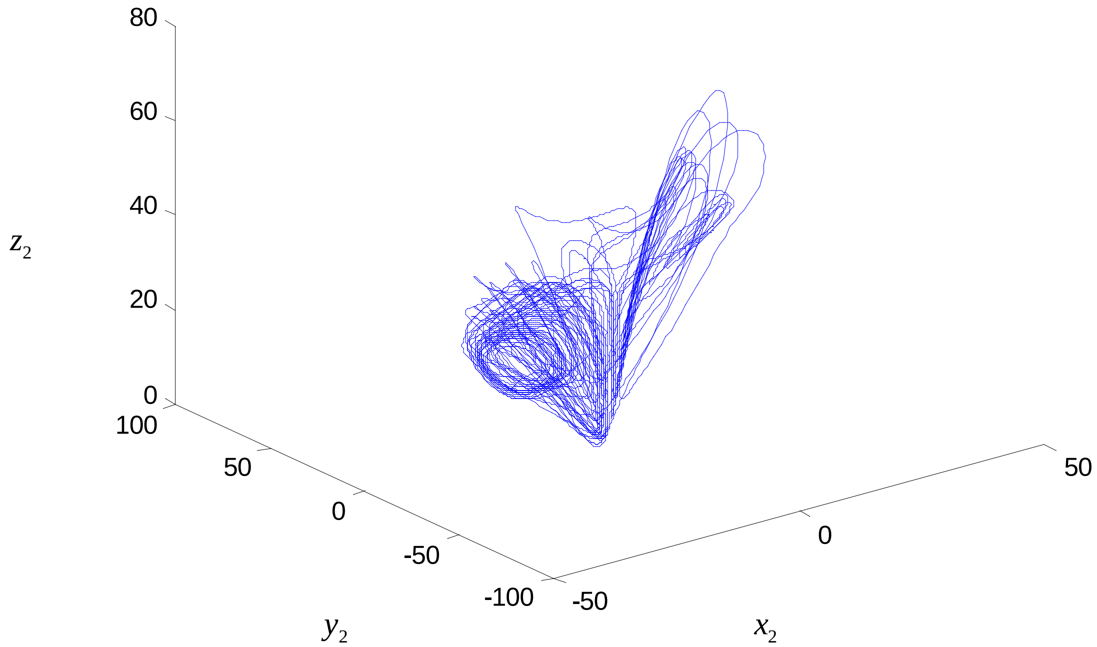

Fig.5. 18 Phase portrait of x_2, y_2, z_2 for $b'(t) = |10y_2 \sin(0.5(\sin(\sin(t))))|$

Chapter 6

Conclusions

We can obtain by different ways hyperchaos of Lorenz system that excited by its own chaos. Chaos control of Lorenz system is achieved by chaos excitation and excitation of sum of chaos and regular functions of time. Chaos synchronization will be obtained by replacing parameter by chaotic and regular function of time. Uncoupled chaos synchronization of two Lorenz systems by replacing parameter by chaotic and regular function.

REFERENCES

[1]. J. M. T. Thompson and H. B. Stewart, Ottino et al., *Nonlinear dynamics and chaos*, Wiley, New York, 2002.

[2]. V.K. Yeragan and R. Rao, "Effect of nortriptyline and paroxetine on measures of chaos of heart rate time series in patients with panic disorder", J. Psychosom. Res., Vol. 55, pp. 507-513, 2003.

[3]. J. M. Ottino et al., "Chaos, Symmetry, and Self-Similarity: Exploiting Order and Disorder in Mixing Process", Science, Vol. 257, pp. 754-760, 1992.

[4]. E.V. Bondarenko and I. Yevin, "Music and control of chaos in the brain", Physics and Control, Proceedings. 2003 International Conference, Vol. 2, pp. 497-500, 2003.

[5]. Huber Aw. Adaptive control of chaotic system. Helv Acta 1989; 343-6.

[6]. S. Celikovsky, G. Chen, "Secure synchronization of a class of chaotic systems from a nonlinear observer approach", IEEE Trans. Automat. Contr., Vol. 50, pp. 76-82, 2005.

[7]. B. Blasius, A. Huppert and L. Stone, "Complex Dynamics and Phase Synchronization in Spatially Extended Ecological Systems", Nature, Vol. 399, pp. 359, 1999.

[8]. O. E. Rössler, "Continuous chaos-four prototype equations", Annals NY Acad Sci, Vol. 316, pp. 376–392, 1979.

[9]. T. Matsumoto, L. O. Chua, K. Kobayashi, "Hyperchaos: laboratory experiment and numerical confirmation", IEEE Trans Circ Syst, Vol. 33, pp. 1143-1147, 1986.

[10]. Y. Li, S. K. Tang, G. Chen, "Generating hyperchaos via state feedback control", Int J Bifurcat Chaos, Vol 15, pp. 3367-3375, 2005.